Chapter 2
Investigating the Freezing of Colloids: Experimental Techniques to Probe Solidification Patterns, Crystal Growth, and Particle Movement

Abstract The freezing of colloids is a complex phenomenon, with multiple, interdependent parameters. A proper observation is thus often the first step towards a better understanding. Many concomitant phenomena take place during the freezing of colloids, related to the growth of the crystals, the redistribution and packing of particles, and the interactions between the front and the particles. Observations and measurements, whether direct or indirect, often provide a first, qualitative and quantitative approach. Such observations are valuable to feed the models developed to predict and understand the freezing of colloids, in particular when they become quantitative. This chapter covers both indirect (force measurement, X-ray scattering and diffraction) and direct methods (light, electron, and X-ray imaging, as well as spectroscopy). The various methods cover a broad range of space and time scales required to completely apprehend the various phenomena of interest.

Keywords Freezing · Colloids · Solidification · Crystal growth · Microscopy · Diffraction · Tomography

2.1 What Are We Looking For?

The freezing of colloids is a complex phenomenon, and the various experimental techniques used for the investigations reflect the variety of features of interest. These features can be classified into four main groups that will determine the techniques that can be used:

- *Solidification patterns*. In many domains, the solidification patterns dictate the properties or behaviour of interest. This is particularly true in geophysics and the study of sea ice and frozen soils (Fig. 2.1), but also in materials science—where the microstructure that results from the solidification pattern controls the properties—or in food engineering. Imaging the frozen system is thus often enough to characterise the pattern. In some cases, you might need a helicopter or a at least a drone, though.
- *Characterisation of crystal growth*. The kinetics and shape of the crystals are often the most interesting features. Direct imaging techniques provide information's

S. Deville, *Freezing Colloids: Observations, Principles, Control, and Use*,
Engineering Materials and Processes, DOI 10.1007/978-3-319-50515-2_2

Fig. 2.1 Pingos (*left*) and melting pingo (*right*) and polygon wedge ice near Tuktoyaktuk, Northwest Territories, Canada. Pingos are mound of earth-covered ice, one of the largest solidification patterns observed naturally, as the pingos can reach up to 70 m in height and 600 m in diameter. By Emma Pike [Public domain], via Wikimedia Commons

about the growth of crystals (morphology, growth kinetics). The crystallographic orientations and orientation textures of the crystals are also investigated and can be the result of a complex interplay of several parameters. Although these were mostly investigated in geophysics, with many studies about the crystallographic characterisation of sea ice and its relation with the environment (temperature, cooling rate, currents), it can also be critical in other occurrences of freezing colloids, and in particular in materials science. Various techniques have been used, including X-ray diffraction, electron backscattered diffraction, or radar measurements in the case of sea ice.

- *Characterisation of the particles behaviour*. Direct imaging techniques provide information about the position, movement, eventually deformation, and packing of the objects. The particle dynamics are often critical to understand the evolution of the systems during solidification. The interaction between particles and the freeze front is a central question in this domain, and its characterisation involves more than direct imaging. Measurements of the force exerted by the particles on the front, as well as the surface charges in the system, are sometimes required. The particles—eventually the crystals too—can have an electrical surface charge. An electrical potential may also appear across the solid/liquid interface. Finally, the organisation of the particles in the frozen body, after their segregation by the crystals, is also of interest in many domains. Because the frozen samples are usually three-dimensional objects, the characterisation of the organisation of particles is difficult.
- *Thermal measurements*. Heat transfer and redistribution play a major role in the freezing of colloids. Heat transfer is critical, as the temperature is usually progressively lowered to induce and complete freezing. The ease and rate at which one may freeze the system, as well as its directionality, are critical. Some solvents, like water, also feature an important latent heat release upon solidification, which may affect the equilibrium of the system. The relative thermal conductivities of the

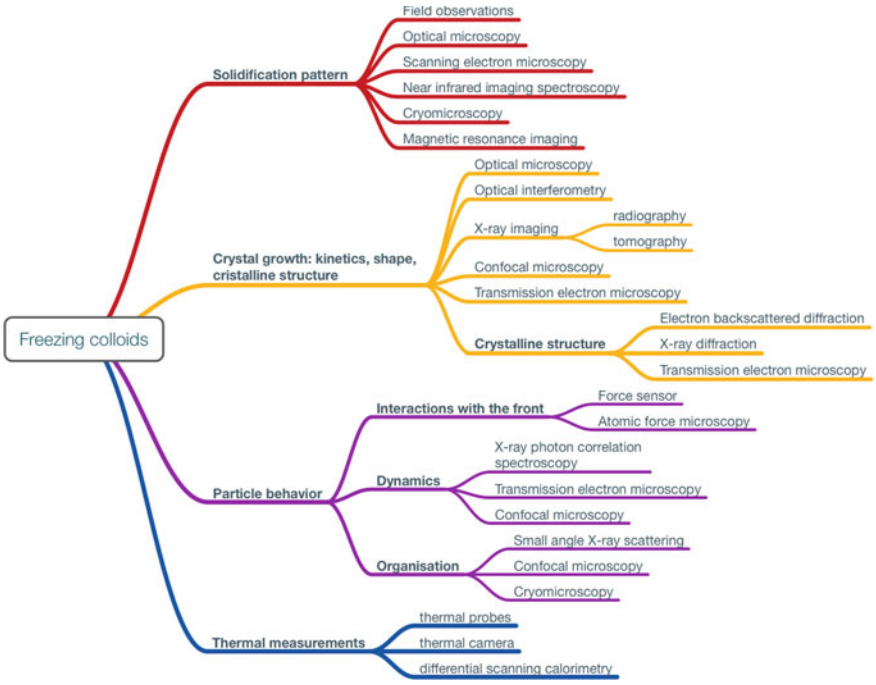

Fig. 2.2 Experimental techniques to investigate freezing colloids and their use

elements (crystals and colloids) can also have a major influence over the evolution of the system, and in particular if they are vastly different. Observing (e.g. with a thermal camera) and measuring the thermal characteristics of the system and its environment is thus also essential. However, very little has been done so far on this aspect. Probes are sometime inserted in the suspension to follow the temperature evolution [1], but little else has been done.

The experimental techniques described in this chapter are listed in Fig. 2.2, along with the information they provide.

This chapter will not cover the techniques used to measure the microstructural features and properties of interest of the materials templated by freezing. These techniques are described along the corresponding properties in Chap. 7.

2.2 Time and Space Scales

There is something unique about the freezing of colloids that is both enriching and problematic for its study and control. The phenomenon and its consequences span almost ten orders of magnitude, from the thickness of the liquid film that separates

the particles and the crystal surface (a few nanometres), to the growth of hills induced by the repetitive freeze/thaw cycles of soils in northern regions, or the long-range alignment of sea ice crystals over hundreds of kilometres. Selecting the appropriate experimental technique therefore strongly depends on which feature we want to investigate.

Observations of the freezing of colloids can provide answers to questions of different nature and characteristics, with a broad range of space and time scales:

- *Understand the particle redistribution organisation* by the freeze front. The scale is that of the particles, often in the colloidal range (submicronic). The interactions between the front and the particles also take place at that range. The scale range is thus in the nanometre to micrometre range.
- *Understand the growth of crystals* and the bulk behaviour of colloidal particles, such as the velocity gradient or concentration profiles. The scale varies from a few micrometres to several hundreds of micrometres, or more.
- *Understand the macroscopic consequences* of the solidification. Depending on the context, the scale can vary from a few micrometres (freezing of thin films) to dozens of metres, in the case of frozen soils investigated in geophysics. The characteristics of the solidification patterns are investigated.

The time scales are variable, but distributed over a much narrower range. The time scale of interest is usually that of crystal growth kinetics and colloidal particle redistribution. An overview of the distribution of space and time scale for the various domains discussed in this book is shown in Fig. 2.3.

The growth kinetics are typically in the $0.1-100\,\mu m/s$ range for most of the occurrences of freezing of colloid, and in the $5-20\,\mu m/s$ range for the usual conditions of materials processing or shaping routes. Ideally, it is thus desirable to track the morphological evolution of crystals and particle distribution within these velocity ranges. This is unfortunately not always straightforward from an experimental point of view.

The underlying mechanisms are characterised by a complex set of interdependent relations. The collective behaviour of particles depends both on the individual interactions between particles and the individual interactions between the particles and the freeze front. The growth morphologies and behaviour are therefore also linked to the particle interactions, and to atomic scale interactions between the different additives present in solution and the solid/liquid interfaces.

Such additives are present for various reasons. They can be impurities initially present in the system; the exact formulation of soils investigated in geophysics is not controlled, unless model soils with controlled formulations are used. The additives can also be added on purpose for processing reasons such as a proper dispersion of the particles. Finally, additives such as crystal growth modifiers can be added to

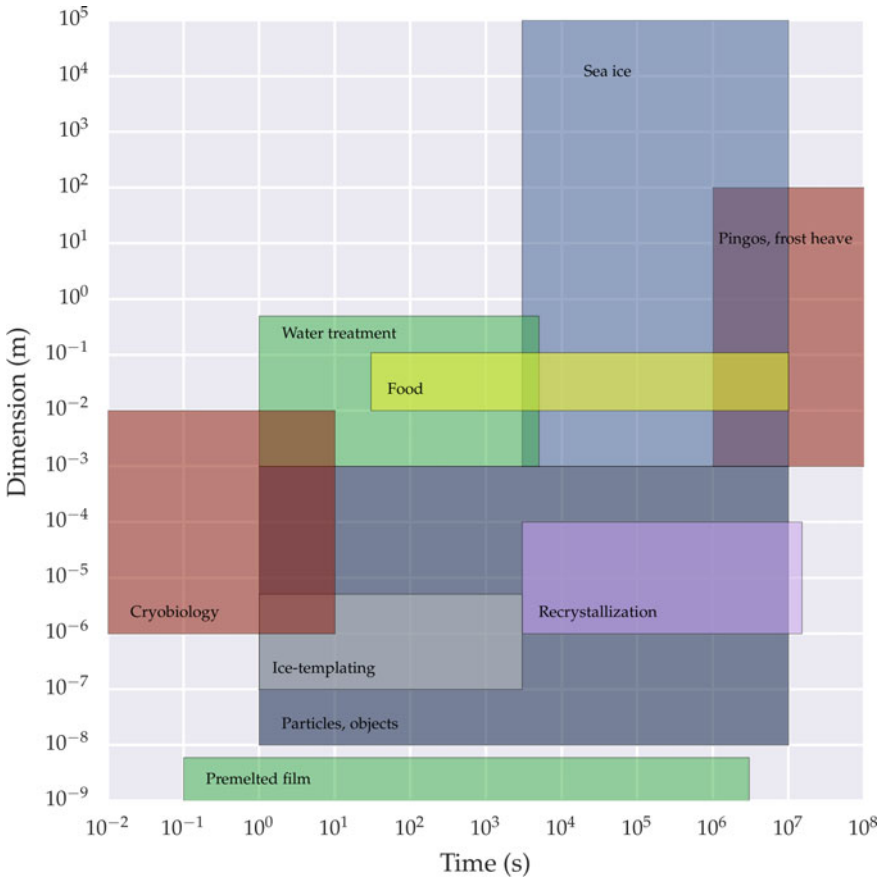

Fig. 2.3 Typical space and time scales of interest in freezing colloids studies. © (2016) Sylvain Deville (10.6084/m9.figshare.4012686.v2) CC BY 4.0 https://creativecommons.org/licenses/by/4.0/

control the growth morphologies of the crystals. These points are all described later in the book.

As usual, the observation can also affect the behaviour of the system. The amount of energy required to modify the behaviour of an individual colloidal particle is relatively small, of the order of $k_B T$. Thermal energy dominates in the colloidal world. The validity of the observations should thus be questioned. If the perturbations induced by optical observations can usually be considered as negligible, the energy brought by a synchrotron X-ray beam can have a dramatic influence on the evolution of the system.

Finally, the behaviour of the system is strongly dependent on small temperature fluctuations. If variations of a few degrees can often be neglected in many instances

of solidification, they can drive drastic changes in the case of colloidal suspensions during freezing.

For all these reasons, many approaches, both direct and indirect, have been tested and used to investigate the freezing of colloids. These techniques cover a broad range of space and time scales.

2.3 Solidification Patterns

The solidification patterns that result from the freezing of colloids are investigated in many domains and cover a broad range of size scales. These patterns are often the first feature of the phenomenon that is characterised.

2.3.1 Field Observations

There are multiple natural occurrences of freezing colloids, such as the freezing of soils or the growth of sea ice in cold regions. A variety of patterns (Fig. 2.4) result from the freezing, such as cells, dendrites, polygons, lenses, and bands, reflecting a wide variety of time and space scales. One of the challenges in the interpretation of such observations is the precise knowledge of the experimental conditions, which greatly affect the freezing behaviour of the system. The investigation of the short- and long-range orientation of ice crystals in lakes or sea ice does not seem to reveal a systematic, reproducible behaviour. The crystalline orientations encountered vary greatly. To ensure a better understanding and reproducibility of the freezing behaviours and patterns, and provide a better chance of understanding the underlying behaviour and assess the influence of the relevant parameters, systematic laboratory experiments, in a controlled environment, have been developed [2], feeding the theoretical developments [3].

The choice of experimental techniques for direct observations reflects both the constant improvement of experimental techniques and the targeted range of time or space scales.

2.3.2 Optical Microscopy

Optical microscopy is an evident choice, for its simplicity: easy to use, low risk of introducing perturbations in the system (little energy is deposited in the sample along the optical path), and appropriate spatial resolution for most of the mechanisms investigated. The main limit to its use is the ability to look only at the surface (Fig. 2.5). With visible light microscopy, it is not possible to look into the bulk of the suspension during freezing. On the other hand, the possibility to finely control the experimental

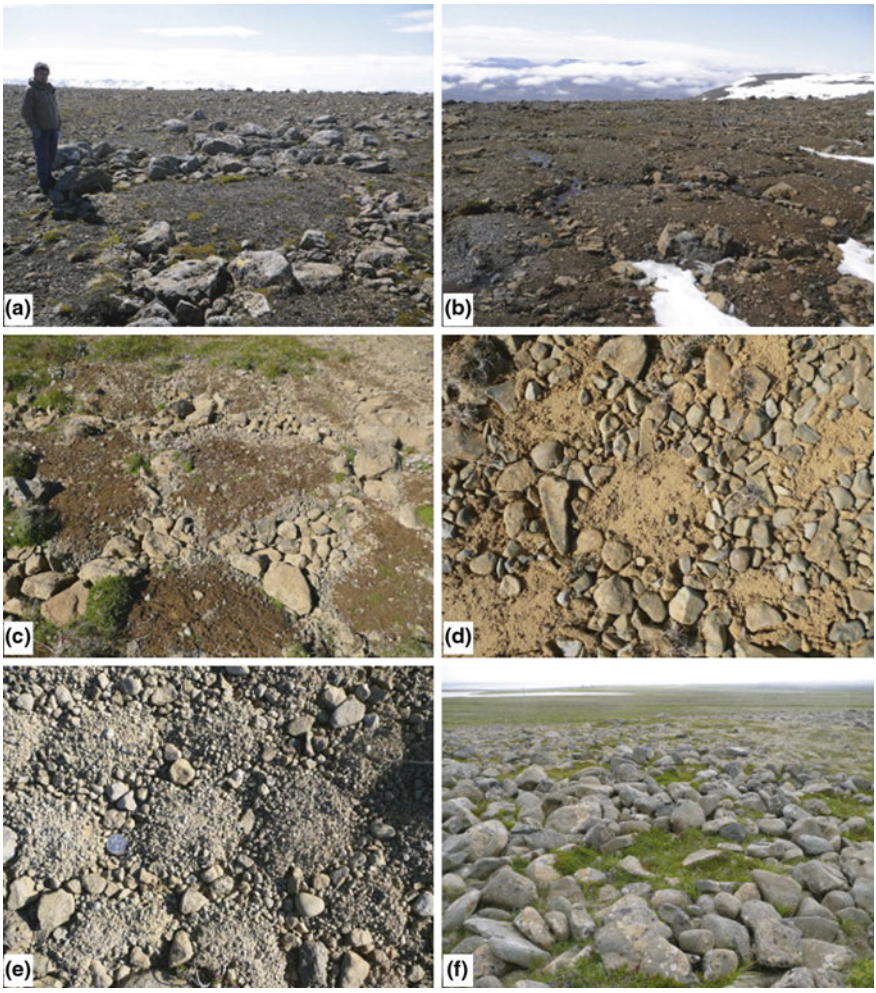

Fig. 2.4 Frozen soils pattern: images of sorted polygons and circle sites, resulting from repeated freezing and thawing cycles. Reprinted from Geomorphology, 139–140, T. Feuillet et al. Classification of sorted patterned ground areas based on their environmental characteristics (Skagafjörður, Northern Iceland), pp. 577–587, Copyright (2012) With permission from Elsevier

freezing conditions (temperature gradient, cooling rate) still makes it a powerful technique.

Optical microscopy was probably the first method used to probe the behaviour of particles during freezing, and in particular to investigate the interactions between particles and crystals. Such experiments [4, 5] were mostly performed to understand the behaviour of a single, isolated particle facing a freeze front. This mechanism is of interest for problems as diverse as the solidification of metals with inclusions [6, 7], or the cryopreservation of cells [8]. Due to technical limitations, the behaviour

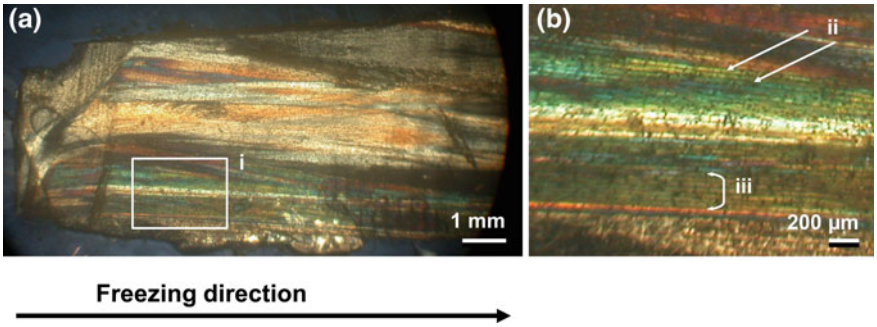

Fig. 2.5 Optical micrograph of a thin, longitudinal section of an ice-templated ice-polymer mixture observed through crossed polarising filters. The lamellar crystals elongated along the freezing direction, as well as the freezing-induced segregation patterns, can be observed at higher magnification (*right*). Reprinted from Materials Characterization, 93, A. Donius et al. Cryogenic EBSD reveals structure of directionally solidified ice-polymer composite, pp. 184–190, Copyright (2014), with permission from Elsevier

of large, millimetre-size particles was first probed, before smaller particles (1–50 µm) were investigated. This shift to smaller particles was driven by both improvements in experimental techniques (spatial resolution) and the broadening of occurrences of freezing colloids [9–11]. Extrapolating the results from such investigations to the behaviour of colloidal particles is not straightforward and suffers from several shortcomings, such as the difficulty of imaging individual colloidal particles and the growing importance of particle interactions in the colloidal size range.

When we are not interested in the behaviour of a single, isolated particle but rather in concentrated particles suspensions, optical microscopy is still a technique of choice, able to yield rich information's. Current work mostly focuses on system with a good control of the freezing conditions (temperature gradient, growth kinetics), which can be obtained in Hele-Shaw cells.

A lot of work was also performed on the directional solidification of transparent alloys such as succinonitrile. Such transparent alloys were developed as analogues for the solidification of metal alloys [12], which could not be easily observed during their solidification because of the high temperature and their opaque nature (among other constraints). Of particular interest in such studies was the behaviour of bubbles [13, 14], often present in melts, and that interact with the freeze front, eventually leading to large defects, as introduced in Chap. 1.

Hele-Shaw Cell

A Hele-Shaw cell is made of two large, parallel plates (as large as 40 cm by 10 cm), separated by a thin gap (2 mm [15–18] or much less) where the suspension is con-

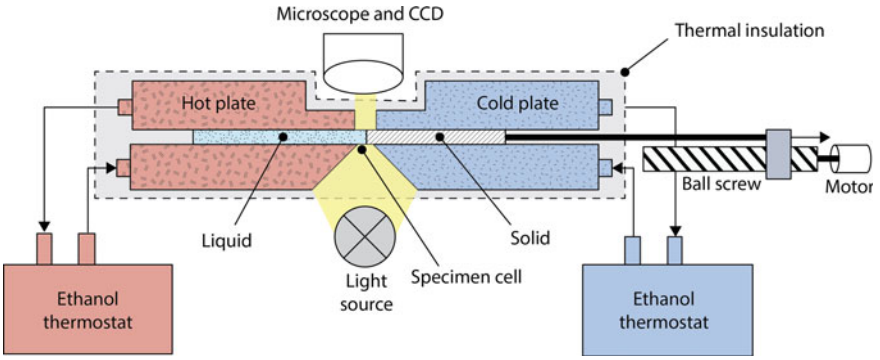

Fig. 2.6 Schematic diagram of horizontal directional freezing stage for optical microscopy. The colloidal suspension is inserted in a Hele-Shaw cell translated through a constant temperature gradient. Both freeze front and temperature gradient can be precisely controlled. Reprinted (adapted) from [17], with the permission of AIP Publishing

tained (Fig. 2.6). A thermal gradient can be precisely applied by two heat exchangers. The cell is then pulled vertically or horizontally (depending on the set-up) at a fixed rate. The freeze front (the isotherms) is therefore always found at the same location, and the growth velocity can be controlled precisely and for long durations. The displacement of the cell is controlled mechanically, the growth regimes can therefore be varied over several orders of magnitude, from 0.1 μm/s to 1 mm/s. It is therefore possible, in particular, to look at growth regimes only obtained after long (hours, or even days) transient regimes. The cell is usually enclosed in a sealed environment, with dry air, which avoids condensation at the surface of the cell. A thermistor can be inserted along the centre of the cell to record the temperature profile. Although not done yet, such set-ups could also be equipped with a thermal camera to provide a precise measurement of the temperature profile. Time-lapse images can be taken with a camera or an optical microscope to track the dynamic evolution of the system.

The surface of the cell is observed with optical microscopy, in reflection mode (Fig. 2.7). It is therefore again not possible to probe the volume of the suspension, but it is nevertheless easy to detect the break-up of the planar freeze front at low growth velocities [19] (Mullins–Sekerka destabilisation) or the growth of dendritic crystals. Since the boundary conditions are well defined, such experiments are useful to validate the developments of mathematical models of freezing colloids such as stability analysis [15, 19–22] or phase field models.

To decrease the uncertainty resulting from surface observations, the thickness of the cell can be reduced down to 20 μm. The Hele-Shaw cell then becomes an almost 2D system. Under such conditions, a single layer of crystals (cells) can be observed (Fig. 2.7). It becomes possible to investigate precisely the morphology of the crystals and the particle redistribution, in particular by looking in transmission mode. If the micron-size particles are used, the individual imaging of particles becomes possible.

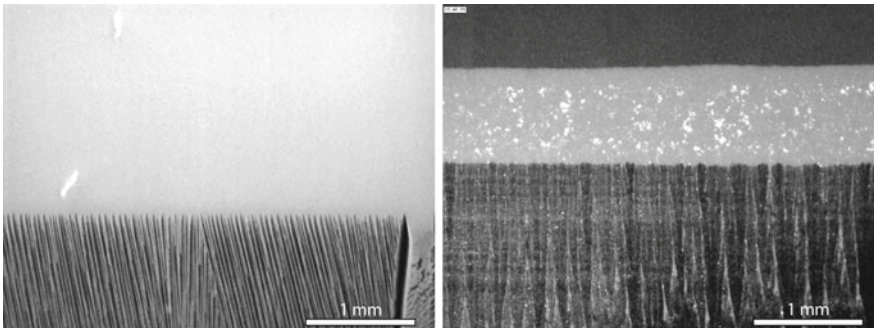

Fig. 2.7 Typical images obtained by optical microscopy and a Hele-Shaw cell. The images were obtained with two different freeze front velocities. Images courtesy of Brice Saint-Michel

To work in transmission mode, the concentration of colloids in the suspension is limited to approximately 10 vol.%.

Even in such a model configuration, the interpretation of the optical microscopy observations is not straightforward and many questions remain. Does segregation of particles occur between the glass sheets? Where are located the particles relative to the crystals (over, under, in front?)? Does the small thickness induce side effects? Bearing in mind these limitations, such experiments are powerful to probe and map the behaviour of freezing colloids under controlled conditions (growth velocity, temperature gradient, colloid concentration, pH).

Hele-Shaw Dual Cells

An Hele-Shaw set-up with two parallel cells, placed under an optical microscope, was used as a differential visualisation method [17, 23, 24]. The two parallel cells are placed in the same temperature gradient. One of the cell is filled with the suspension, while the corresponding pure solvent is placed in the other one (Fig. 2.8). The comparison of the interface position in the two cells, combined with the knowledge of the temperature gradient, provides a precise (± 0.01 K), quantitative measurement of the interfacial undercooling [17, 24] (Fig. 2.9), difficult to obtain otherwise. The undercooling finds its origin in the kinetics of solidification and the presence of particles and additives found in the solvent.

Optical microscopy suffers from two limitations: the small depth of view, and the light scattering by the suspension, which both limit the spatial resolution and the maximal concentration of particles that can be investigated. However,

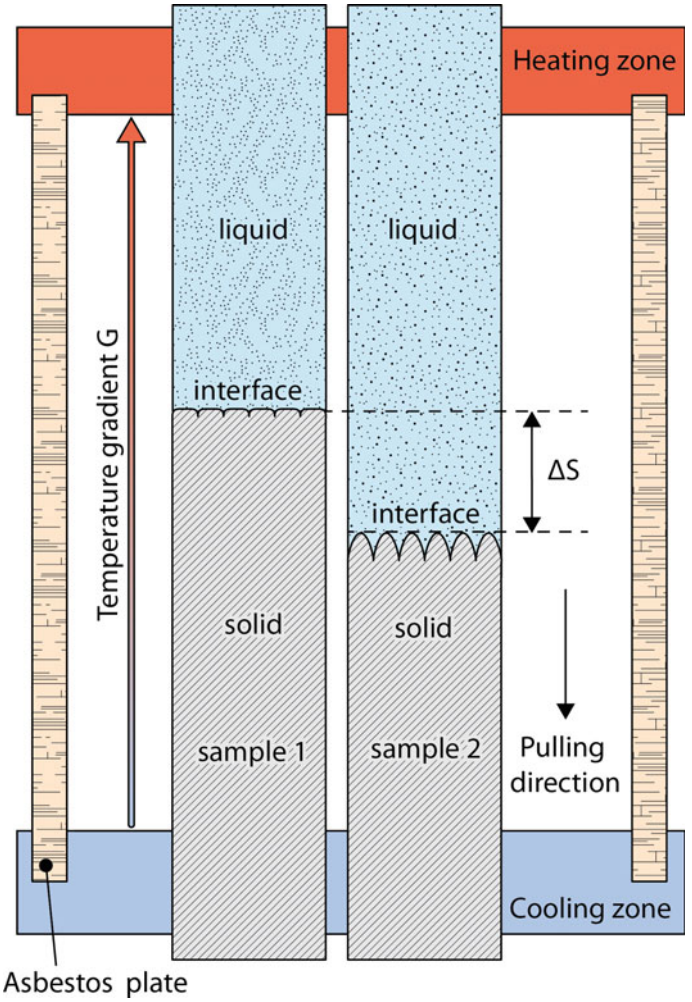

Fig. 2.8 Schematic representation of the experimental set-up for the Hele-Shaw cell with the differential visualisation method. ΔS indicates the interface gap between the two samples. The knowledge of the gap and the temperature gradient provides a precise measurement of the undercooling. Reprinted (adapted) from [17], with the permission of AIP Publishing

the excellent control of interface velocity (imposed externally) and temperature gradient (also imposed externally), along with a rapid image acquisition, render them extremely valuable.

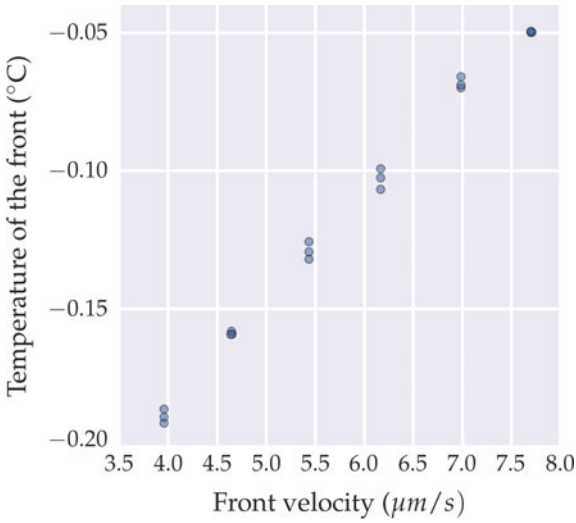

Fig. 2.9 Relation between interface undercooling and interface velocity, measured with the differential visualisation method, for a temperature gradient of $G = 8.72$ K/cm, an initial volume fraction $\phi_O = 10\%$, and polystyrene particle diameter 100 nm. Three separate experiments were performed demonstrating a good reproducibility. After [17]

2.3.3 Scanning Electron Microscopy

A solution to the limited depth of view and spatial resolution of optical microscopy is the use of scanning electron microscopy (SEM). In conventional SEM, a high level of vacuum is applied to the specimen chamber. The environment is therefore dry and liquid samples cannot be observed, direct imaging is not possible.

In the environmental mode of SEM, a partial water pressure in the microscope specimen chamber let one observe liquid or wet samples. The electron gun is still under vacuum, but the column is divided into several subunits with different partial pressures. In the specimen chamber, the partial water pressure is such that liquid samples can be observed [25].

If the sample is placed on a Peltier stage, it is possible in principle, by exerting a proper control of the temperature and pressure conditions, to freeze a suspension while looking at it.

In practice, it is difficult to achieve a proper control of the freezing conditions. In preliminary experiments (A. Bogner et al., unpublished), freezing was achieved but the growth rates were rapid. It was not possible to image the intermediate freezing stages and the growth of ice crystals. The crystal growth and particle redistribution was nevertheless similar to that obtained in the laboratory when freezing colloidal suspensions (Fig. 2.10).

A better control of the freezing conditions was obtained by leaving the specimen chamber opened while freezing (the sample is therefore at ambient pressure), but the intermediate stages cannot be imaged. It was nevertheless possible to image the sublimation of the ice, revealing the organisation of particles repelled by the freeze front. These first experiments were not conclusive regarding the benefits of ESEM for the in situ investigations of freezing of colloids. Ferrer et al. [26] were more

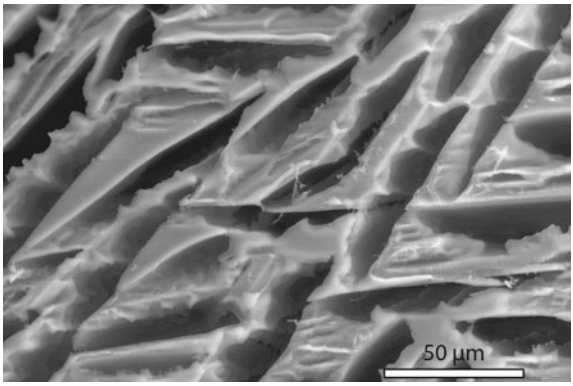

Fig. 2.10 In situ freezing in an environmental SEM. A colloidal suspension made of alumina particles in water was frozen using the Peltier stage and imaged directly in the SEM. Lowering the pressure can then evaporate the ice. The porosity visible here corresponds to the space left by the sublimated ice crystals. Achieving a good control of the freezing is difficult. Image courtesy of Agnes Bogner

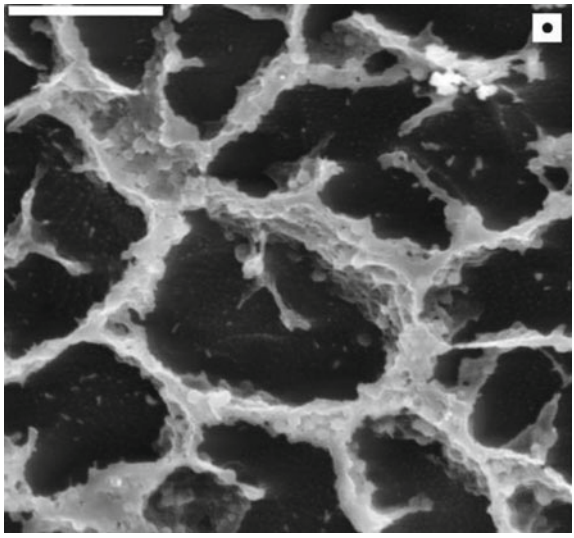

Fig. 2.11 Cryo-etch SEM of a binary colloidal system composed of 290 nm particles dispersed within the aqueous silica gel and frozen with liquid nitrogen (scale bar: 5 µm). Reprinted with permission from [26]. Copyright (2006) American Chemical Society

successful with the approach, and developed a *cryo-etching technique* to investigate the formation of hierarchical assembly of liposomes by freezing binary colloidal systems. Freezing was performed out of the microscope. The frozen sample is then put into the scanning electron microscope. A proper setting of the temperature and pressure can trigger sublimation of the ice, thus revealing the frozen assembly of colloids (liposomes, and/or silica gels) (Fig. 2.11).

A different approach was used by Donius et al. [27]. A frozen sample (ice/polymer in this case), was frozen ex situ, and introduced in the microscope, on a cold stage

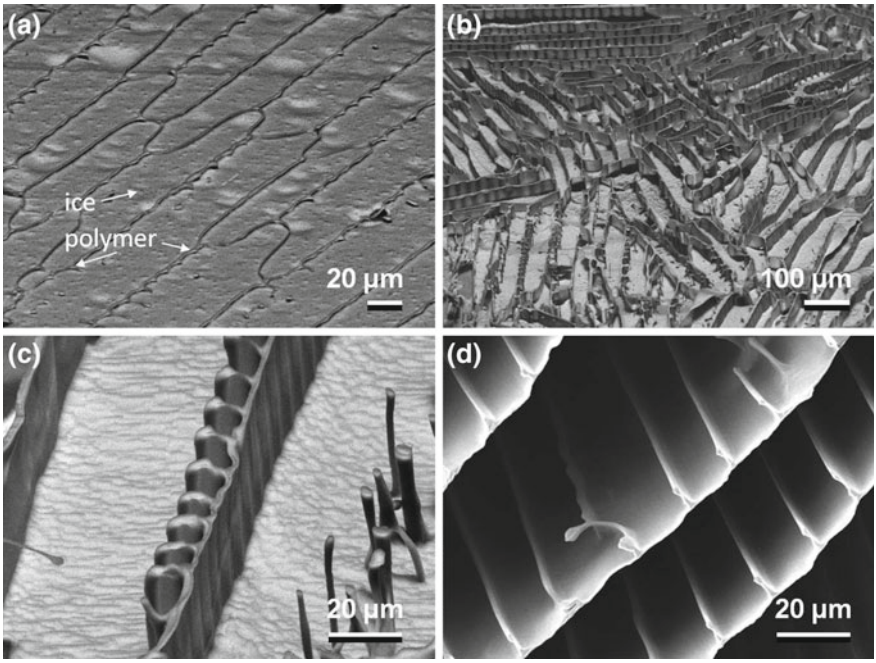

Fig. 2.12 Frozen ice/polymer structure observed in scanning electron microscope, after some sublimation of the ice. The dendritic surface features, aligned along the freezing direction, are visible. Reprinted from Materials Characterization, 93, A. Donius et al. Cryogenic EBSD reveals structure of directionally solidified ice-polymer composite, pp. 184–190, Copyright (2014), with permission from Elsevier

held at −120 °C. Because of the reduced pressure in the chamber (between 8 and 17 Pa), the ice started to sublimate, revealing the organisation of the ice-templated polymer (Fig. 2.12). This approach was used to do in situ electron backscattered diffraction (EBSD), described p. 73.

2.3.4 Magnetic Resonance Imaging

Magnetic resonance imaging (MRI) is a spectroscopic technique based on nuclear magnetic resonance. It is originally a medical imaging technique, but has been used to investigate water dynamics and fluid transport in porous solids, and in particular in construction materials [28], frozen food [29], or sea ice [30, 31]. Of particular interest in these studies is the freeze/thaw behaviour, and the monitoring of freezable water during these cycles, which provide information's regarding the resistance to degradation of the materials (in particular concrete). MRI has also been used to look at the microstructure of ice-templated materials, such as bioactive hydrogels [32].

The imaging is based on the absorption and emission of radio frequency energy when the materials are placed in an external magnetic field. The hydrogen atoms, for example, because of their moment, can partially align when an external magnetic field is applied. When the magnetic field is removed, the atoms oscillate while returning to equilibrium, emitting a radio signal. This signal is measured in MRI. MRI is particularly suited to look at the relaxation properties of hydrogen atoms, and is thus often used to image water in a material. It is thus particularly appropriate to investigate water and/or ice distribution in materials or tissues.

MRI is a tomography imaging technique. It can thus give access to the three-dimensional structure or phase repartition of materials. There is a great potential for investigating the topics of interest discussed in this book, although MRI equipments are not really standard pieces of equipment in materials science laboratories.

2.3.5 Near-Infrared Imaging Spectroscopy

A novel technique to observe ice crystals was developed by combining a micro-slicer unit and a near-infrared spectral imaging unit [33]. Near-infrared spectroscopy methods are routinely used in food engineering or agriculture to evaluate the quality of products. The absorption bands of water are different, which results in a contrast in spectral imaging. The micro-slicer unit is used to reveal the successive cross sections through the sample investigated, a three-dimensional reconstruction can then be performed (Fig. 2.13). The imaging resolution and the precision of the slicing thickness are similar (a few micrometres). Although primarily developed for food engineering investigations, to reveal the growth and morphology of ice crystals in biological materials, the technique could be directly applied to investigate frozen colloidal suspensions. The absorption bands of the colloids will be different from that of water and ice, offering an additional source of contrast.

2.3.6 Cryomicroscopy

Cryomicroscopy only shares a similar name with ESEM. Cryomicroscopy is largely used by biologists [34], chemists [35], geophysicists, or food engineers. It allows observation of hydrated samples without destroying their structure. In materials science, it was used to look at silica or latex particles suspensions, investigate the hydration state of cement, look at the flocculation of clay [36], characterise the structure of gels, or investigate the freeze/thaw resistance of latex paint [37] (Fig. 2.14).

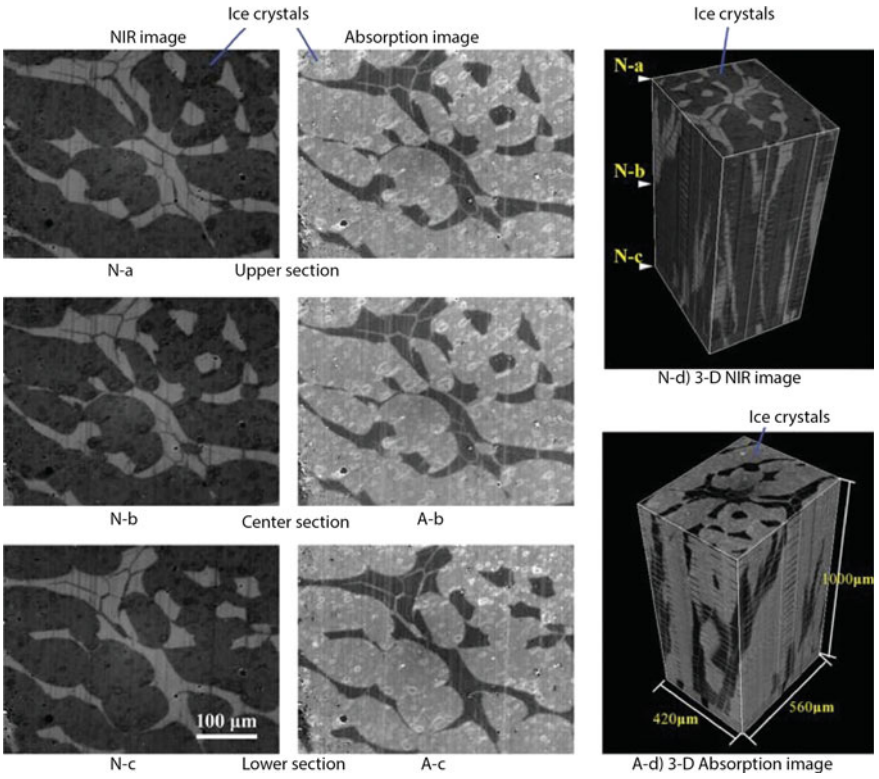

Fig. 2.13 Near-infrared imaging spectroscopy: observation of ice crystals in a beef sample. From: Three-Dimensional Measurement of Ice Crystals in Frozen Materials by Near-Infrared Imaging Spectroscopy, G. Do et al. Drying Technology, 33, pp. 1614–1620 (2015). Reprinted by permission of the publisher (Taylor & Francis Ltd, http://www.tandfonline.com)

Cryomicroscopy is the combination of high-pressure freezing and scanning electron microscopy. Freezing is obtained by a high-pressure freezing set-up, the only one able to create amorphous ice over a typical thickness of 200 µm without the use of antifreeze compounds. The fast ice growth rate is achieved by a combination of a rapid cooling rate (10^3 K/s or faster) and a high pressure. The objective here is to fix the sample (suspension, tissue, gel) in its initial state without degrading or modifying its structure. In the case of colloidal suspension, cryomicroscopy can be used to investigate the dispersion state of the suspension without modifying the spatial organisation of the particles [38]. Once frozen and sublimated, the sample is moved into the specimen chamber of a regular scanning electron microscope where it can be observed at high resolution, under vacuum (or not).

Studer et al. [39], for instance, investigated the state of water in a bovine cartilage. The estimated cooling rate required to create amorphous ice over 200 µm was found

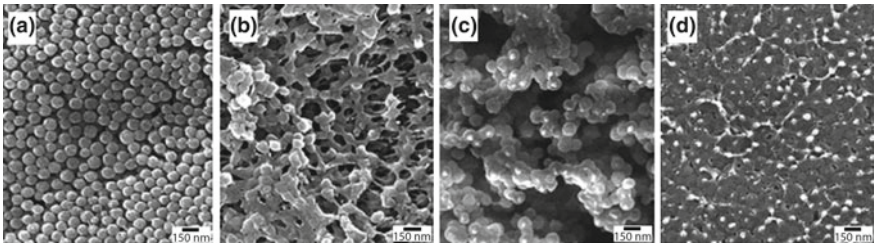

Fig. 2.14 Cryomicroscopy observations to investigate the stability of latex paint against freeze/thaw cycles. Images of the same latex, which contains only 0.5 wt% of PEG, after freezing and/or thawing at different rates. **a** Fast freezing in liquid ethane (−88 °C). **b** Fast freezing under high pressure in liquid nitrogen (−196 °C) and then thawed slowly overnight. **c** Slow freezing in a freezer at −18 °C. **d** Slow freezing in a freezer at −18 °C and then slowly thawed overnight. From Journal of Coatings Technology and Research, 3(2), 2006, pp. 109–115, C. Zhao et al. © OCCA 2006. With permission of Springer

between 10^3 and 10^5 K/s, which is a good indication of the growth rate typically achieved with the technique.

The cooling rate and freeze front velocities required by cryomicroscopy make the observation of transient phenomena impossible. In the case of freezing colloids, the growth rates are too rapid to result in any particle redistribution, which is usually the phenomenon of interest. It can be nevertheless used to obtain information about the dispersion state of colloidal suspension that will be frozen [38].

2.4 Crystal Growth: Kinetics, Shape, Crystalline Structure

The solidification patterns that develop during freezing are a direct consequence of the growth behaviour of the crystals. Investigating the growth kinetics, morphologies, as well as the crystalline structure of the crystals is thus critical in many domains. These investigations cover again a broad range of size scales, although the crystals are often in the micrometre range (1–100 μm), and the growth kinetics in the micrometre per second range (1–100 μm/s). Because the freezing system is often out of equilibrium, the energy brought by the experimental observations must be carefully considered. This can be particularly critical with X-ray imaging techniques and transmission electron microscopy.

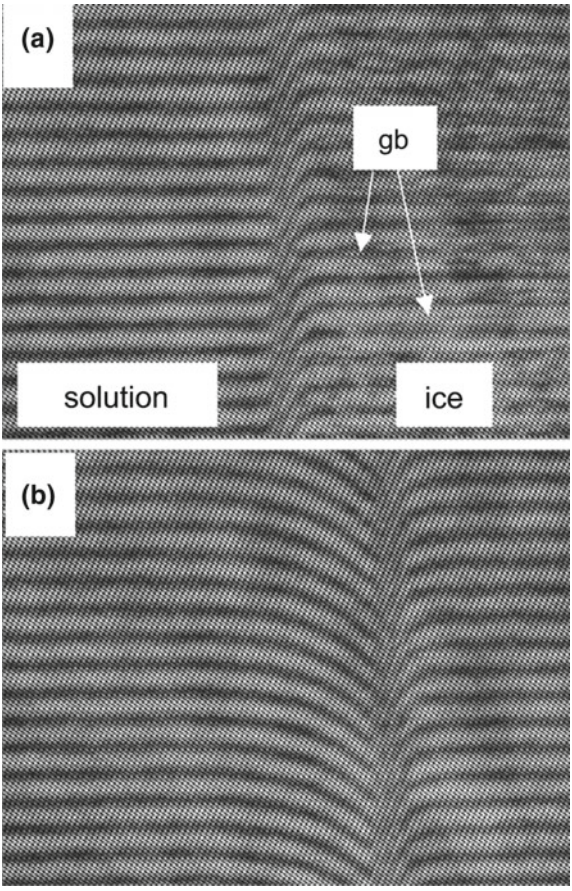

Fig. 2.15 Optical interferometry: interference fringe profile in a bovine serum albumin solution grown with a planar ice/solution interface at 2 μm/s **a** before initiation of ice growth and **b** during quasi-steady state growth. A similar fringe curvature is observed in the ice phase at all times. Reprinted with permission from [40]. Copyright (2002) American Chemical Society

2.4.1 Optical Interferometry

Optical interferometry can be used to measure locally the concentration of solutes, in particular around a freeze front. This approach has not been used for freezing colloids yet, but has been applied to investigate the freezing behaviour of aqueous solutions such as water–protein or water–glucose systems [40] (Fig. 2.15). It is possible to measure precisely the solute concentration gradient around the interface, a measure difficult to obtain otherwise. The sensitivity to concentration of optical interferometry is better than that of X-ray imaging (described below), for which an important difference of absorption coefficient is required to obtain enough contrast. Optical interferometry could thus be of great interest to investigate the freezing of colloids. It should nevertheless be noted that light must pass through the sample. It will thus be necessary to work with small sample thickness and low concentration of particles.

2.4.2 X-Ray Imaging

X-ray imaging, and in particular X-ray computed radiography and tomography, are powerful techniques to probe the structure of materials and the dynamics of several phenomena. The basis of X-ray imaging relies on the differential absorption of X-ray by different phases (Fig. 2.16). The detector (a scintillator) converts the X-ray adsorption signal into a visible light image, which is then magnified by optics and recorded by a high speed CCD camera. The resolution and acquisition times of synchrotron beamlines (Fig. 2.17) are better than that of tabletop or laboratory tomographs. In the case of colloidal suspensions, X-ray are particularly suitable since the absorption coefficient of water (or ice) and inorganic colloids such as ceramic oxides are vastly different.

Several imaging modes are possible:

- in *radiography*, the viewing angle of the sample is kept constant. The signal on the detector is the result of the X-ray beam attenuation through the thickness of the sample. Although the 3D structure of the sample cannot be obtained from such

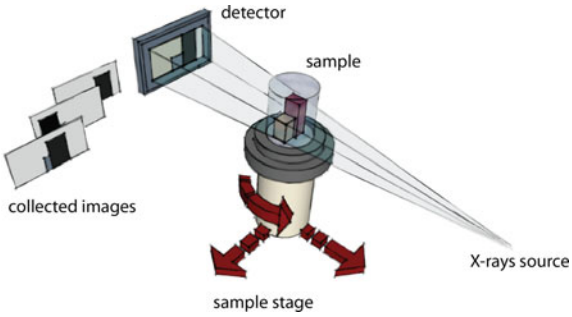

Fig. 2.16 Principles of X-ray computed tomography. © (2016) Sylvain Deville (10.6084/m9.figshare.4012707.v1) CC BY 4.0 https://creativecommons.org/licenses/by/4.0/

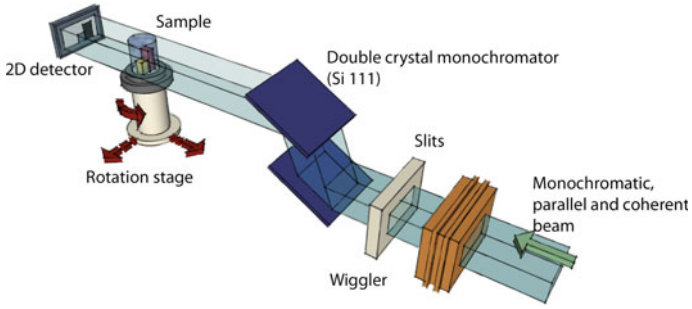

Fig. 2.17 Typical set-up of synchrotron X-ray imaging at the beamline. © (2016) Sylvain Deville (10.6084/m9.figshare.4036059.v1) CC BY 4.0 https://creativecommons.org/licenses/by/4.0/

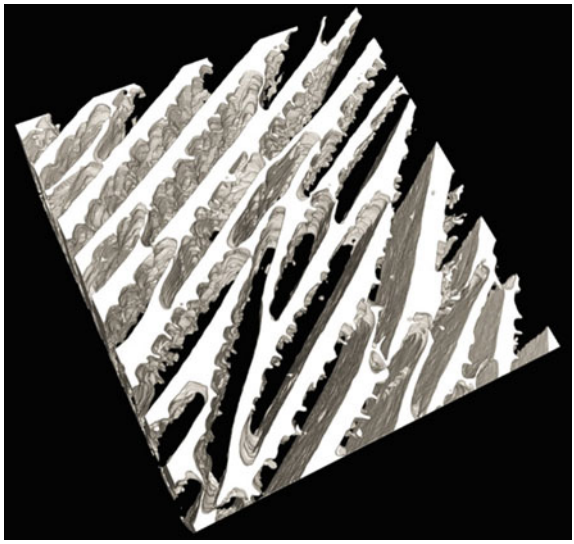

Fig. 2.18 Typical three-dimensional reconstruction of an ice-templated ceramic obtained by X-ray tomography.

experiments, it is nevertheless a powerful technique to probe rapid phenomena if the sample has a 2D morphology or a rotational symmetry. This is the case of the unidirectional freezing of colloids in a capillary. The freeze front can be easily located, so that its position with time can be tracked.

- in *X-ray computed tomography*, several hundreds (or thousands) of radiographs are acquired at different viewing angles, over 180°, by rotating the sample. This set of radiographs can be computed to reconstruct the 3D attenuation map of the X-ray beam. Spatial resolutions down to 10 nm can now be achieved at synchrotron sources. This can be particularly useful to reconstruct the 3D morphologies of the ice crystals and the phase comprising the concentrated particles between the ice crystals (Fig. 2.18).

X-ray imaging solves two limits of optical microscopy techniques: the impossibility to look through nontransparent samples (most materials are transparent to X-ray), and the three-dimensional, non-destructive imaging of the sample. It is thus possible to look in situ at crystal growth in a concentrated colloidal suspension of metal oxides particles.

The acquisition rates of 3D images were too low to probe dynamics for a long time, with typical exposure times of several minutes to several hours. A combination of X-ray radiography, to probe the dynamics of the freeze front, and X-ray computed tomography, to obtain a 3D description of the crystals and concentrated particles phase, can provide many insights into the phenomenon and has been used several times [41–47]. Such experiments can also be conducted on laboratory scale with commercial laboratory X-ray sources [48].

The set-up required for the imaging is not demanding. Three main conditions must be satisfied:

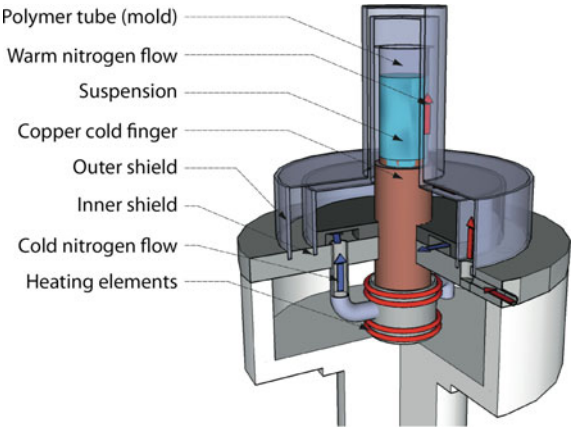

Fig. 2.19 Set-up for in situ X-ray imaging of freezing colloids. The copper cold finger is cooled by liquid nitrogen. The warm nitrogen flow between the two polymeric cap prevents condensation and freezing at the surface of the mould, which could induce artefacts by progressively increasing the absorption of the beam. Reprinted from S. Deville et al. Journal of the American Ceramic Society, Wiley [43] © 2009 The American Ceramic Society

- We must be able to cool the suspension. Unidirectional solidification is preferred. This can be achieved either by liquid nitrogen cooling or with Peltier plates. The temperature required is not very low, as the freezing of colloidal suspensions usually starts a few degrees below 0 °C.
- The enclosure comprising the suspension must be transparent to X-ray while not degrading too rapidly under the beam.
- Condensation, leading to ice deposition, must be avoided, although this might not be critical since ice is transparent to X-ray (if the thickness of the ice deposit is small).

A typical example of a cell developed for such imaging is shown in Figs. 2.19 and 2.20.

Many commercial solutions are available, as several companies specialise in devices for X-ray imaging experiments.

X-ray imaging of freezing colloids nevertheless suffers from several shortcomings. The main issue is related to the adsorption of X-ray by the colloids, which may lead to a local increase of temperature. For regular X-ray imaging, the flux of high-energy X-ray is not high enough to trigger such problems. For rapid imaging, short exposure times ($1/1000^{th}$ of a second) are required. The flux of high-energy X-ray is therefore high, and the temperature can locally increase by several degrees [49]. This increase is large enough to affect the growth of ice crystals.

A side effect of the drastic increase of acquisition frequency is the enormous volume of data generated. A typical 3D reconstruction represents a volume of several hundreds of megabytes. The acquisition of several 3D tomographs per second can therefore rapidly generate terabytes of data. Even though storing such amount of

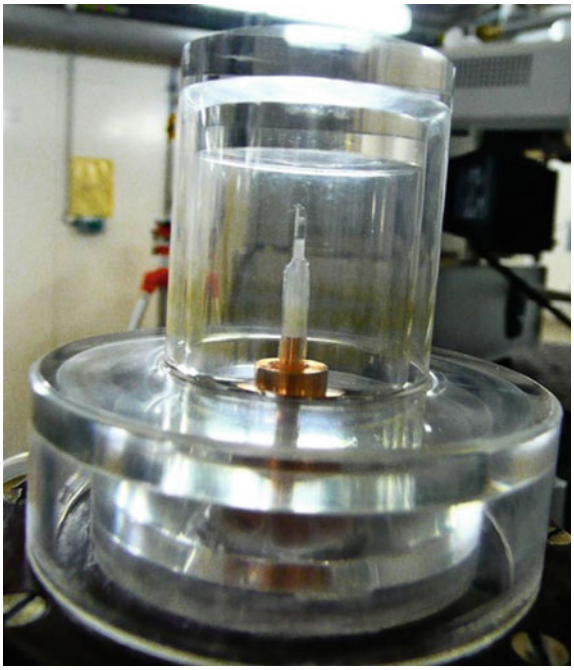

Fig. 2.20 Picture of the cell used for X-ray imaging. The suspension (*white*) can be seen in the capillary inside the straw

data is not a problem anymore, thanks for the advances in computing, the treatment and reconstruction of the data is key in these experiments. In addition, beyond making pretty pictures, the quantitative description of three-dimensional morphologies requires specialised concepts, tools, and software. Many open-source software such as ImageJ [50], Fiji [51], or Python and one of its many image analysis libraries [52], have been developed to assist such analysis, making them more accessible today.

Recent progresses in acquisition rates, with faster and more sensitive detectors, allows for rapid imaging. 3D tomographs can now be acquired with a frequency of a few Hertz. For systems with a slow dynamics, such as a freeze front moving at a few micrometres per second, a time-lapse, three-dimensional reconstruction (Fig. 2.21) has been achieved [49]. The actual three-dimensional morphology of the ice crystals can be characterised. However, the intensity of the beam is high (4×10^{13} photons $(\mathrm{s} \cdot \mathrm{mm}^2)^{-1}$). The adsorption of the beam in such conditions can be problematic. The samples under irradiation by the beam get a heating rate of 2 °C/s, leading to local heating of the suspension of a few degrees, inducing thus growth artefacts (the tip radius of the crystals is sensitive to the local temperature gradient).

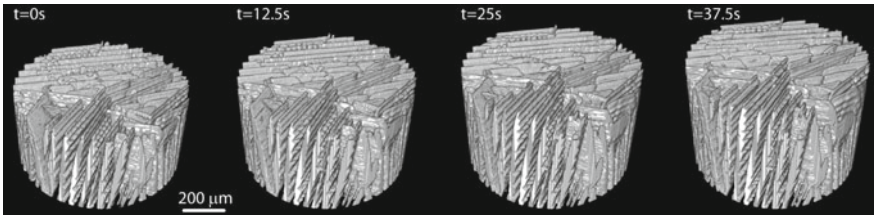

Fig. 2.21 Fast tomography imaging of ice crystals growing in a colloidal silica suspension. Time-lapse sequence during freezing (12.5 s between each image). The acquisition time of each image is approximately 1.5 s. Reprinted from Acta Materialia, 61(6), S. Deville et al., Time-lapse, three-dimensional in situ imaging of ice crystal growth in a colloidal silica suspension, pp. 2077–2086, Copyright (2013), with permission from Elsevier

X-ray imaging is now a suitable solution for describing both qualitatively and quantitatively the growth and morphologies of ice crystals. The spatial resolution is nevertheless not sufficient yet to describe the three-dimensional arrangement of colloidal particles. It is probably a safe bet to assume that it is only a matter of time (a few years) before we can do it.

2.4.3 Confocal Microscopy

Confocal microscopy is a ubiquitous technique in life sciences. The ability to provide a clear, optical sectioning of samples provides unparalleled information's about the structure and mechanisms of living organisms. Its use in materials science is much less popular, although promising [53].

In optical microscopy, areas above and below the focal plane contribute to the image, which results in a typical blur. In confocal microscopy, a pinhole, located between the specimen and the detector, is used to select only the signal coming from the focal plane (Fig. 2.22). The resulting image is thus sharper. By taking a series of optical slices from different levels in the sample, it is thus possible to access to 3D observations. It can thus be used as an optical microscope with an extended (quasi infinite) depth of view.

In laser scanning confocal microscopy, the point-by-point illumination with the laser can be used to trigger fluorescence in the sample, whether natural or coming from fluorophores. If colloidal particles with a fluorescent core are used, it becomes thus possible to characterise the three-dimensional organisation of a network of particles [54]. This has been extensively used in the soft materials community [55–57] to investigate the phase transitions of colloidal suspensions.

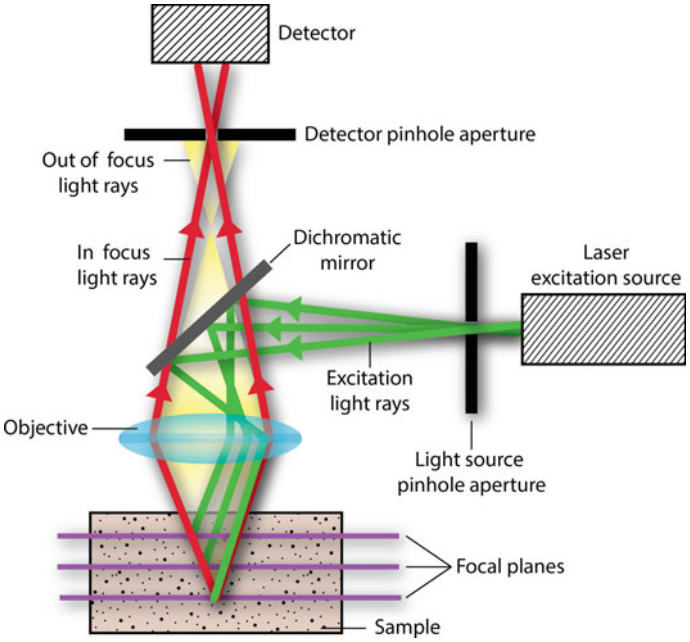

Fig. 2.22 Principles of confocal microscopy. Only the light emitted from the focal plane passes through the detector pinhole and reaches the detector. The out of focus light rays are eliminated. By moving the focal plane vertically and collecting the light, a three-dimensional reconstruction of the emitted light with a narrow focal depth can be collected

Combined with appropriate cold sources (Peltier stage), confocal microscopy seems like an ideal technique to investigate freezing colloids. The addition of a small amount of fluorescent dye to the suspension allows for simultaneous imaging of the solvent and the particles, at two different wavelengths. The spatial resolution currently achieved (submicronic) by confocal microscopy systems makes them suitable to observe colloidal suspensions.

Very few reports of confocal microscopy applied to freezing colloids can be found, though. Ma et al. [58] applied it to ice-templating, but to investigate the homogeneity of a composite material (collagen/chitosan), and not to investigate the in situ freezing mechanisms. Biswas et al. [59] used confocal microscopy to investigate the spatial organisation of colloidal particles into clusters, resulting from the growth of ice crystals, and compared these structures to the output of Brownian dynamics modelling.

Marcellini et al. [60] developed a confocal microscopy procedure to follow in situ the time-lapse growth of ice crystals. The imaging contrast is achieved by the addition of a fluorophore to the aqueous solution (Fig. 2.23). During freezing, the fluorophore

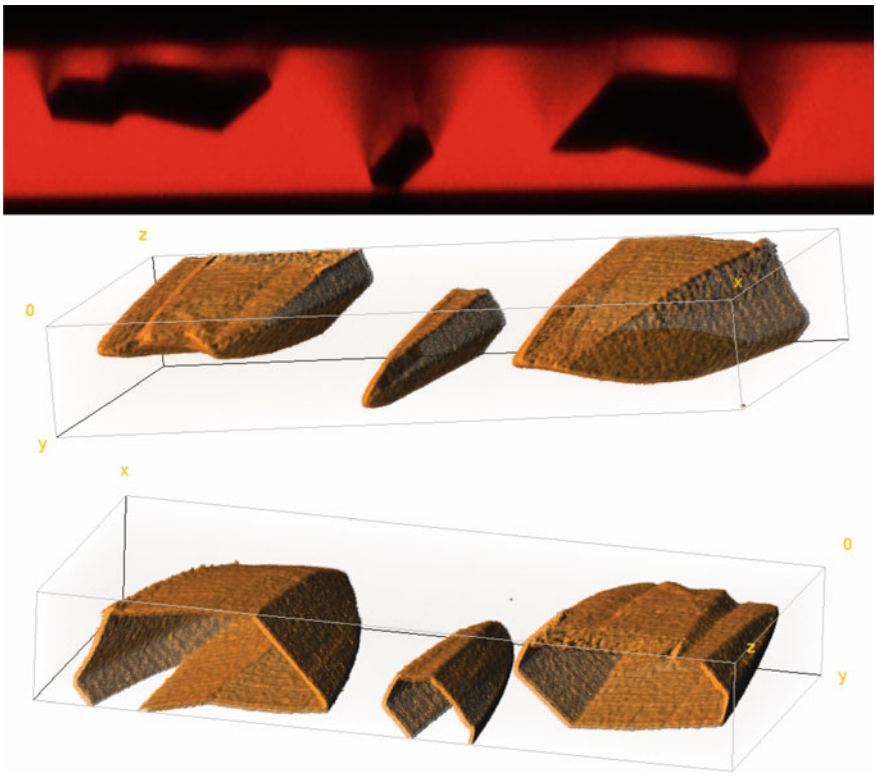

Fig. 2.23 Typical confocal microscopy image of ice crystals growing in an aqueous solution that contains a fluorophore (Sulforhodamine B, here). The *red* corresponds to the liquid water, the *black regions* in the centres are the crystals. Shadowing effects due to the crystals can be observed in the upper part. Cross-section dimensions: 260 μm by 60 μm. The three-dimensional reconstruction of the crystals surface is shown in the lower picture (front view and back view) (Colour figure online)

segregates from the crystals. The acquired images can then easily be segmented and reconstructed into three-dimensional images. Using fluorescent particles also makes it possible to image each individual particles and their trajectory and packing between the crystals (Fig. 2.24). Such observations should certainly provide new insights into these phenomena, at the particle scale.

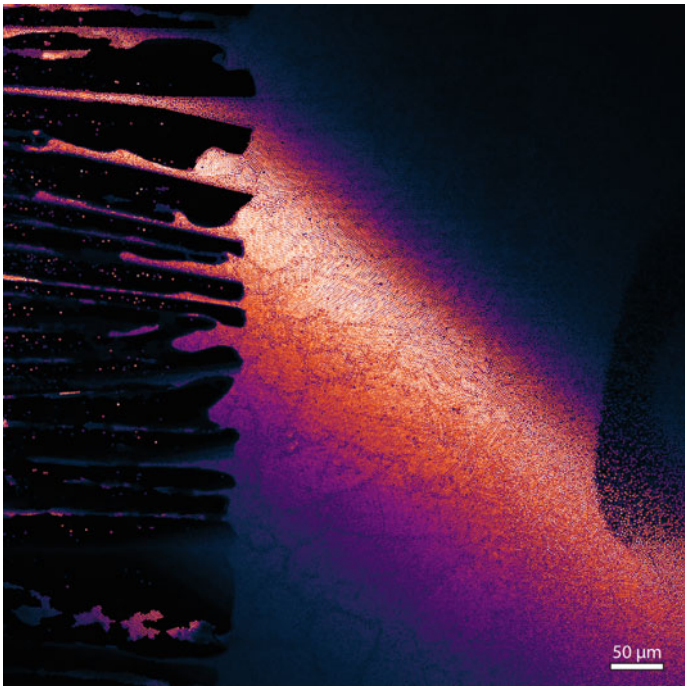

Fig. 2.24 Typical confocal microscopy image of ice crystals growing in a colloidal suspension of fluorescent particles. The crystals, growing from the left to the right, segregate and concentrate the particles. A dense layer of concentrated particles can be seen in front of the crystals. Image courtesy of Juliette Maria

Despite its huge potential, confocal microscopy has never been used to far to investigate in situ the freezing of colloids. The possibility to image the particles, the crystals, and the solvent simultaneously is nevertheless appealing. The space (submicron resolution) and time scale (up to several images per second) are relevant to the typical dynamics found in freezing colloids situation, and in particular in ice-templating. As opposed to the X-ray tomography techniques described below, little energy is deposited along the optical path. Artefacts due to the technique are therefore less likely. Finally, the latest technical developments provide video-rate imaging possibilities, which enable the capture of the typical crystal growth and particles dynamics.

2.4.4 Transmission Electron Microscopy

Advances in transmission electron microscopy (TEM) during the last decades opened the door to observations of liquid samples in controlled environments (atmosphere, partial pressure). Several techniques have been developed, such as environmental TEM [61] or scanning TEM (STEM) [25]. In the context of freezing colloids, TEM could be a powerful approach to investigate the nucleation and growth mechanisms, and more precisely the crystal structure (through in situ diffraction), or defects formation at the nanoscale. It may also provide imaging of the interaction of the ice front and nanoparticles, which cannot be obtained by optical microscopy.

Several challenges await those tempted to do TEM while freezing colloidal suspensions. Technical issues, related to the precise control of the atmosphere, or the influence of the beam, must be overcome. High density currents can induce local heating and interact with the samples, and drive electromigration of particles [62]. The volume expansion of the sample in the cell (when water is used) must also be taken into account.

Only such TEM study can be found [63] (Fig. 2.25). The stage developed for in situ freezing was made of a copper rod attached to a cold reservoir at 150 K (ethanol) or 77 K (liquid nitrogen). A Pt resistance provided heating to regulate the temperature, controlled by a thermocouple. Low beam current density was used to minimise heating and interactions with the sample. The liquid sample was enclosed in a 300–500 nm thick cell, with SiN_x windows.

In spite of the limitations discussed above, these observations demonstrated the potential of the approach, providing direct observations of 30 nm Au nanoparticles interacting with the freeze front (Fig. 2.26). The crystal structure of ice (hexagonal or cubic in that case) could be determined in situ from the diffraction patterns. The displacement of a particle over a limited distance before engulfment was reported, a behaviour quite unexpected for this range of particle size. Artefacts associated with the cells, such as the adhesion of nanoparticles to the window, or a possible inclination of the interfacial plane, render the quantitative interpretation of the observations complex for now.

Bearing in mind the limitations and artefacts induced by the beam and the cell, TEM is a promising technique for investigating freezing colloids.

2.4.5 Electron Backscattered Diffraction

Electron backscattered diffraction (EBSD) is extensively used in materials science to measure locally the crystal orientation in microstructures. Although it is most commonly used in ceramics and metals, it can also be applied to ice crystals, provided that the temperature and pressure conditions can retain the ice crystals in a stable structure.

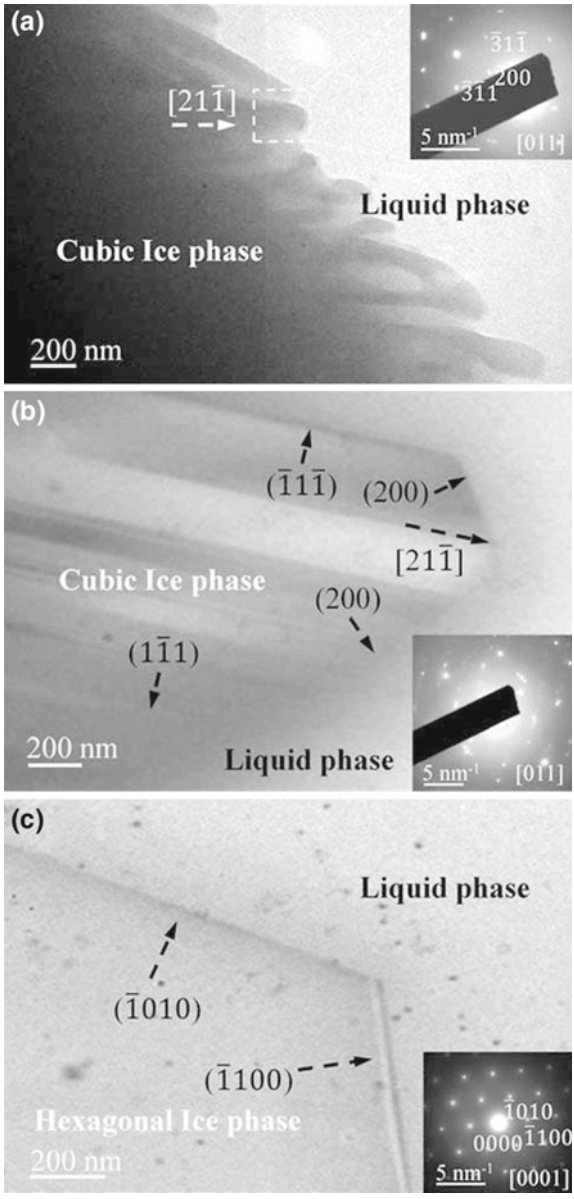

Fig. 2.25 In situ TEM while freezing colloidal suspension: bright field images. Cubic (**a**, **b**) and hexagonal (**c**) ice crystallisation at 220, 245, and 260 K. The corresponding selected area electron diffraction patterns (SAED) are shown in insets. The diffraction patterns and images are aligned such that the crystallographic direction in the image is aligned with that in the diffraction pattern. The arrows indicate the primary crystallographic orientations. From K. Tai et al. In situ cryogenic transmission electron microscopy for characterising the evolution of solidifying water ice in colloidal systems, Microscopy and Microanalysis, 20, 330–337, 2014. Reproduced with permission

Progresses in environmental scanning electron microscopy, which rendered observations under partial pressure possible, have made EBSD on ice crystals possible. Although EBSD cameras are now commonly found in laboratories, the combination of EBSD, environmental conditions, and a cold stage (usually a Peltier stage) to

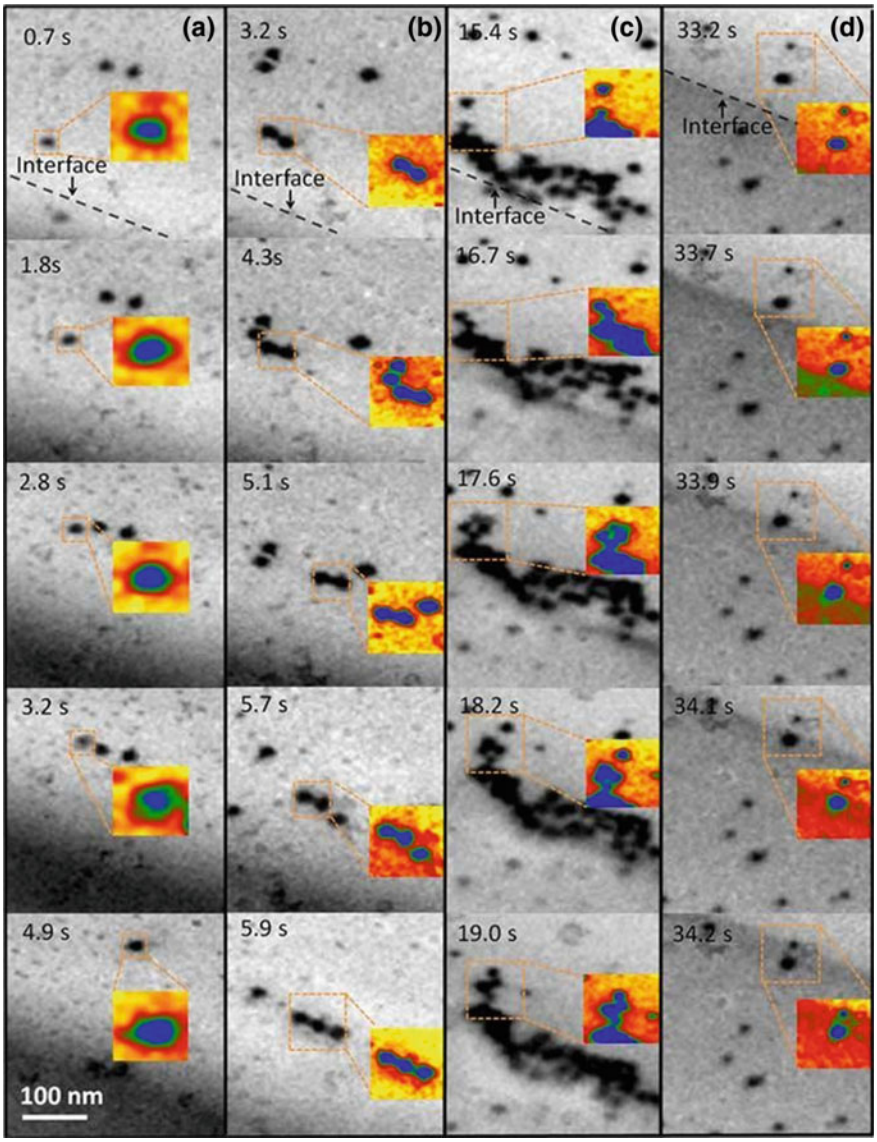

Fig. 2.26 Time-lapse bright field transmission electron microscopy images showing the redistribution of gold nanoparticles by the advancing hexagonal ice/water interface at 260 K. The four sequences illustrate different behaviours. **a** An individual particle is pushed by the long-range interaction. **b** Strong attractive particle–particle interactions. **c** Agglomerate of particles repelled by the interface. **d** A nanoparticle is first repelled by the ice/water interface over a limited distance (40 nm) before engulfment by the solidification front. From K. Tai et al. In situ cryogenic transmission electron microscopy for characterising the evolution of solidifying water ice in colloidal systems, Microscopy and Microanalysis, 20, pp. 330–337, 2014. Reproduced with permission

freeze and maintain the crystals at low temperature,[1] is still a rare combination, and few studies can be found.

Cryogenic EBSD appeared first around 2005, and has been the domain of ice physicists thus far [64–66], interested in the microstructure and properties of ice [67, 68] (and in particular creep and grain growth), and its phase transformation, which are relevant in a number of domains, from geophysics to biology and astrophysics. The reader interested in the procedures may refer to Prior et al. [69], for the current state of the art of sample preparation and acquisition techniques. Among the authors' conclusions is the difficulty of preparing samples with air entrapped (bubbles) or hard particles. Cryogenic EBSD on frozen colloidal suspension remains thus a challenge today.

Only two studies [27, 69] reported cryogenic EBSD on frozen colloids system (Fig. 2.27), in the water/chitosan and water/alumina systems.

In the first case, the *c*-axes of the ice crystals were oriented perpendicular to the direction of the temperature gradient (Fig. 2.27). The *a*-axes laid along the solidification direction. These results were in contradiction with the in situ XRD performed on frozen colloidal suspension of zirconia [70]. A more diverse crystallographic orientation was found in the second study (Fig. 2.28).

A side benefit of the technique is the possibility to sublimate some of the ice at the surface of the sample, which reveals the templated structure of the frozen system, as illustrated previously (Fig. 2.12). An EBSD camera is not required in this case.

2.4.6 X-Ray Diffraction

X-ray diffraction (XRD) is uniquely suited to investigate the phase transitions in materials science. It can therefore be used to investigate the growth of ice crystals, which occurs in freezing colloids situations. Although only minimal equipment is required, few studies of ice characterisation in the presence of colloids can be found. The growth behaviour and characteristics of ice, on the other hand, have been heavily investigated, in particular in Earth science and geophysics.

Almost any XRD set-up can be upgraded with a cooling cell for a moderate cost. Cooling cells are now commercially available (Fig. 2.29). The stage is typically cooled by vaporised nitrogen pumped through the cell. It is therefore possible to perform directional freezing.

Only the surface of the sample can be investigated, though. Low temperature XRD can thus be used to capture crystallographic features of ice crystals when they reach the surface of the sample. If the environment of the sample is not controlled, condensation from the atmosphere and the formation of a surface layer of ice can occur rapidly (within a few minutes or less) and must be avoided. However, standard

[1] The samples can also be frozen externally and transferred to the observation chamber with a cryo-transfer system.

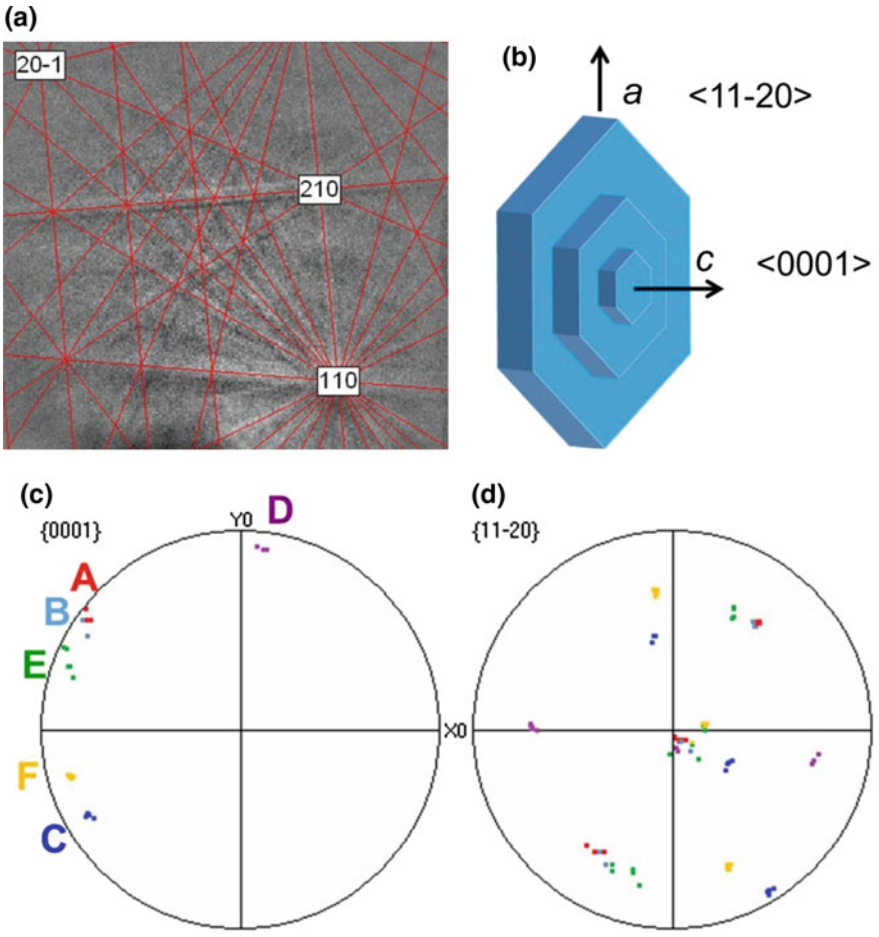

Fig. 2.27 EBSD on frozen ice/polymer structure observed in scanning electron microscope. **a** Typical EBSD pattern from the centre of an ice lamella. *c*-axis 0001 (**c**) and *a*-axis 11–20 (**d**) pole figures for 23 ice crystals sampled in six different domains. Reprinted from Materials Characterization, 93, A. Donius et al. Cryogenic EBSD reveals structure of directionally solidified ice-polymer composite, pp. 184–190, Copyright (2014), with permission from Elsevier

XRD machines are rapid enough to capture the data before artefacts due to the condensation appear.

In the context of freezing colloids, low temperature XRD can provide numerous important information:

- *the crystallographic orientation* of the ice crystals. This is still an open issue. One study reported *c*-axis aligned along the direction of the temperature gradient [70], and another one the opposite result [27]. Understanding how the crystals orient, the role of not only the freezing conditions (cooling rate, supercooling, directionality)

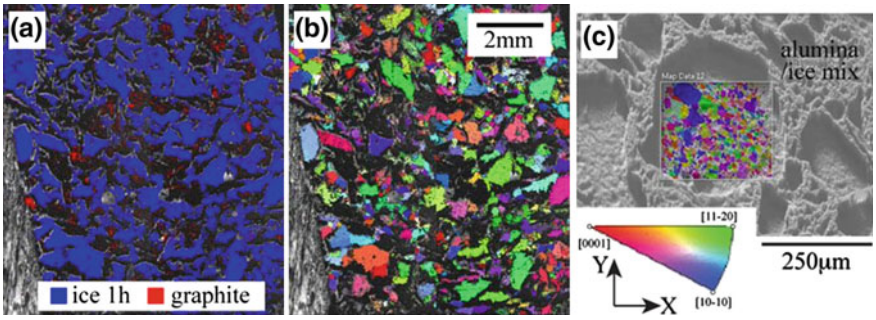

Fig. 2.28 Large area EBSD phase map of sample comprising a graphite mix (20 vol% graphite), deformed unconfined at −7 °C, $2.5 \times 10^{-6} s^{-1}$ strain rate to a strain 0.1. The *uncoloured pixels*, not indexed, correspond mostly to graphite. **b** EBSD map of the same area as shown in **a**. The *colour* indicates the orientation of the ice crystals. **c** Frozen suspension of alumina prepared by mixing ice with 20%, 300 nm alumina. Reprinted from D. Prior et al. Journal of Microscopy, Wiley [69] © 2015 The Authors (color figure online)

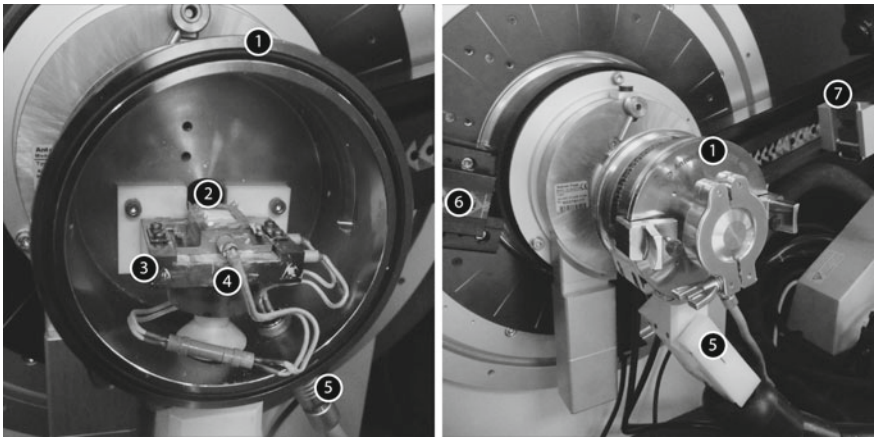

Fig. 2.29 Cold stage used for low temperature X-ray diffraction. The stage is cooled by vaporised nitrogen. The vaporised liquid nitrogen circulates through the tube (*5*). Legend: (*1*) sample chamber, (*2*) sample, (*3*) cold stage (metallic support), (*4*) thermocouple, (*5*) cold nitrogen supply, (*6*) X-ray source, (*7*) X-ray detector. © (2016) Sylvain Deville (10.6084/m9.figshare.4036065.v1) CC BY 4.0 https://creativecommons.org/licenses/by/4.0/

but also of the colloids and the additives used, would be an important milestone in many topics.

- *the measurement of residual stresses*. The shifts of the peaks could be used to estimate the pressure resulting from the water-to-ice transformation (volume increase) [71]. The accommodation (or not) of freezing-induced stresses is important in many situations, and in particular in ice-templating where the rigidity of the mould seems to control, to some extent, the formation of defects in the frozen struc-

ture and thus in the final materials. The properties of the mould affect of course the accommodation of residual stresses. Varshney et al. [71] used synchrotron XRD to measure the stress at the growing water/ice interface, and found the stresses to be equivalent to an hydrostatic pressure of 2–3 kbars.

2.5 Particle Behaviour

Direct observations in real space remain the most common approach of investigating the features that develop during the freezing of colloids and in particular the particle behaviour. Many space and time scales can be probed with direct observations. The interpretation of the observations is usually easier than that of indirect techniques.

Three types of information are sought:

- Quantifying the interactions between the particle and the front. As described in the next chapter, many analytical models have been developed to predict and understand the behaviour of particles facing a freeze front. Quantitative measurements of these interactions are useful to validate or invalidate these models.
- Investigate the particle redistribution by the freeze front. Are the particles engulfed? Repelled? Temporary repelled? Do they reorganise into agglomerates? Remain isolated?
- Investigate the organisation of particles in the frozen structure.

2.5.1 Force Measurements

The growth of crystals in a dilute suspension triggers particle redistribution. This redistribution can be induced by a direct interaction with the freeze front, can be the result of collective movements of particles by diffusion, or can be the result of individual steric or electrostatic interactions of particles. The interaction between a single particle and a freeze front, described in more details in the next chapter, generally results in the application of a force on the particle. The sum of forces applied on the particle will then determine its fate—rejection or encapsulation—eventually accompanied by a modification of the local freeze front morphology. The experimental measure of the force applied on the particle by the interface therefore provides useful information to qualify and quantify these interactions.

Force Sensors

Ideally, the interaction between a single isolated particle and the freeze front should be measured. Some of the first experiments were performed on millimetre glass beads, fixed on a tungsten wire attached to a force sensor [72] (Fig. 2.30). The conditions are nevertheless far from that encountered during the freezing of colloids. In particular, the surface/volume ration is different from that of colloids. It is thus difficult to assess

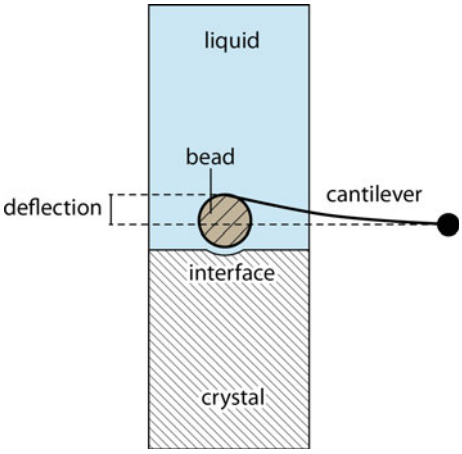

Fig. 2.30 Measure of the force exerted by a solidification front on an isolated single bead. The deflection of the cantilever is measured, providing thus the value of the force exerted by the solidification front on the bead

precisely the role of surface charges or surface chemistry. The gravity effects do not affect the measure since the particle is attached to the sensor. The experiments were limited to a specific condition where the freeze front is planar. When not attached to a sensor, the particles are either encapsulated or repelled. The situation with a cellular interface, more complex in terms of possible configurations but also more representative of most freezing colloids situations, has not been investigated.

When the particle is attached, intermediate behaviours such as a temporary rejection by the interface over some distance before engulfment occurs cannot be investigated.

Many parameters have nevertheless been investigated. The simplicity of the set-up and the measures provides flexibility in terms of materials system: nature of the solvent, particle size, surface chemistry. Several solvents have been investigated: naphthalene, camphor, salol, and succinonitrile. The chemistry of the glass beads surface was also changed by chemical treatments, and the role of additives (such as methylene blue) to the solvent was investigated. The forces measured were of the order of 10^{-5} N, for particles with diameter in 0.4–1.67 mm range (Fig. 2.31).

The motivation for these experiments was to validate (or invalidate) the theoretical predictions of the critical freeze front velocity (that defines the shift of behaviour between rejection and encapsulation), which mostly depends on the particle size. These models and predictions are discussed in Chap. 3.

Atomic Force Microscopy

The behaviour of smaller, colloidal particles has been investigated by atomic force microscopy [73]. The set-up is similar to the force sensor experiments: a spherical silica particle is attached to the tip of the atomic force microscope (Fig. 2.32). The tip is then dipped into a water or colloidal suspension droplet that is frozen from below, by a Peltier stage. The technique provides a precise measure of not only the force exerted on the particle by the freeze front, but also the direction along which the

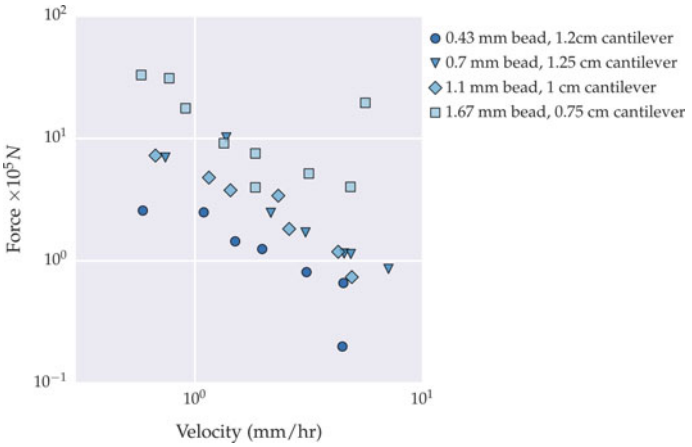

Fig. 2.31 Measure of the force exerted by a solidification front on an isolated single particle. Average values of force versus bead diameter for naphthalene. The force exerted by the interface increases with the bead size, but decreases with the front velocity. Data from [72]

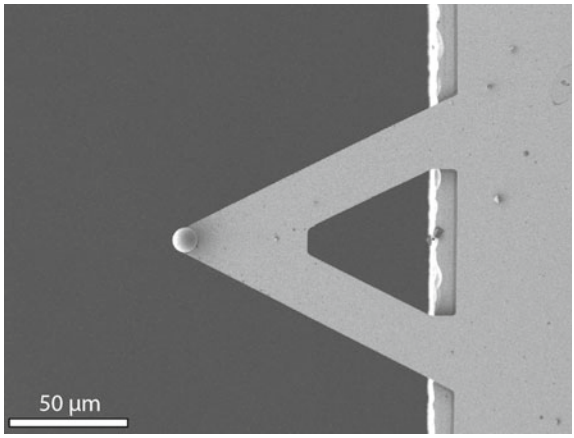

Fig. 2.32 Atomic force microscopy tip with a 10 µm silica particle glued at the extremity. Image courtesy of Gisele Lecomte-Nana

force is applied (Fig. 2.33). This angle information can be extracted from the flexion and torsion of the cantilever, which are both measured. When the sample is thawed, the cantilever retrieves its original position. Additional information may be extracted from this movement too. Although different behaviours have been observed, depending for instance on the pH, or the dispersion state of the suspension, the interpretation of the measurements remains difficult. A number of hypotheses are required, such as the exact morphology of the freeze front, which is unknown. The freeze front velocity, known to have a critical influence on the behaviour of the particle, is also unknown. The control of the freezing conditions is difficult.

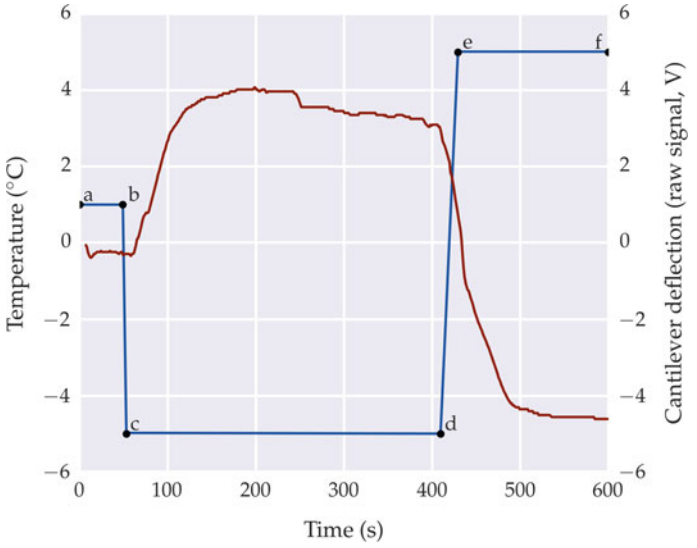

Fig. 2.33 Atomic force microscopy measurements of the interaction between a particle and a freeze front (ice). Temperature profile (*blue*) and deflection signal (*red*). Cantilever reactions: **a**–**b** equilibrium, **b**–**c** repulsive impact, **c**–**d** equilibrium, **d**–**e** energy release upon melting, **e**–**f** equilibrium. After [73] (colour figure online)

2.5.2 X-Ray Scattering and Spectroscopy Techniques

Instead of tracking the behaviour of individual particles, X-ray techniques such as X-ray photon correlation spectroscopy (XPCS) or small angle X-ray scattering (SAXS) can probe the dynamic behaviour of a large number of colloidal particles. The use of X-ray gives access to length scales comparable to the size of the individual colloidal particles, and time scales relevant to characterise the collective behaviour of colloids during and after freezing.

SAXS provides a representation in the Fourier space of the distribution of mass within the probed sample, at the length scale of one to several particles. It is therefore a useful technique to characterise the redistribution and arrangement of particles induced by the freeze front, averaged over a large number of particles. We can determine if particles are in close contact or not, and measure the particle radius.

X-ray photon correlation spectroscopy (XPCS), on the other hand, can be used to probe the dynamics of particles encapsulated in ice. XPCS can probe slow dynamics at the nanometre scale in the bulk, and is thus ideally suited to investigate phenomena like the dynamics of colloidal particles in ice. Like X-ray computed tomography, XPCS can probe opaque samples. In principle, unlike for soft matter of biological materials, X-ray damages are not an issue in frozen colloidal systems.

The crystals concentrate particles, whose ballistic motion can be described by a Stokes–Einstein diffusivity. The autocorrelation function of the azimuthally averaged

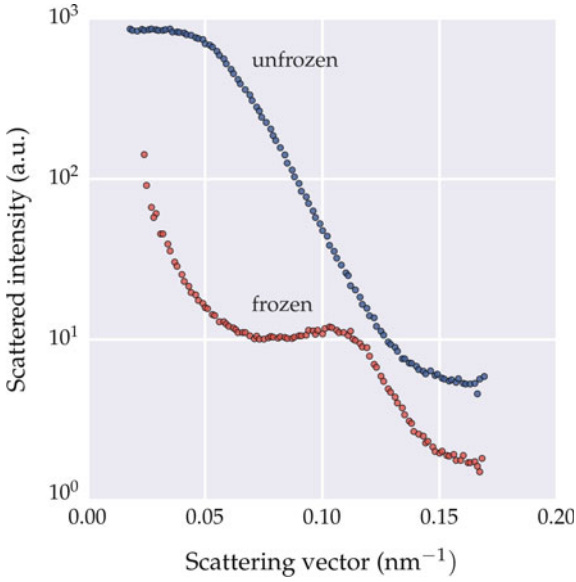

Fig. 2.34 Small angle X-ray scattering of unfrozen and frozen colloidal suspension. SAXS intensity versus scattering vector. After [74]

intensity $I(q, t)$ gives access to the dynamics of the particles (Fig. 2.34). The length scale of these dynamics is directly related to the scattering vector. A proper adjustment of the scattering vector and exposure time gives access to the relevant range of space and time scales.

These techniques can be coupled with video microscopy. Such coupling, which provides a direct observation of the formation of aggregates, is helpful to understand the scattering and spectroscopy results.

Such experiments [75] were performed on 7 vol.% suspensions of 32 et 300 nm silica particles. These characteristics are closer to that encountered in the natural occurrences of colloid freezing, such as the growth of sea ice. If a complete interpretation of the results is not trivial and depends on several assumptions, these experiments are potentially valuable to describe the spatial distribution of particles after freezing. It was proposed, in particular, that the motion of grain boundaries in polycrystalline ice moves the entrapped colloidal particles around. Such mechanisms are important to understand in situations where frozen structures are kept at low temperature for a long time (ice cream, frozen soils).

Two of the experimental techniques described previously in this chapter are also particularly promising to investigate the particle behaviour during freezing: transmission electron microscopy and confocal microscopy. Optical microscopy is also relevant, although its interest to characterise the behaviour of colloidal particles is limited by its spatial resolution, the extended depth of view, and light scattering.

2.6 Thermal Measurements

The temperature gradient and its evolution as the system is cooled is important to understand the solidification behaviour and patterns. Three parameters are essential to control:

- the freezing point of the suspensions. It depends on the formulation used, and in particular the presence of additives and solutes.
- the cooling rate, which controls the freeze front velocity (and thus the periodicity of the solidification pattern)
- the temperature gradient(s), which control the directionality of crystal growth and thus of the solidification pattern. The latter is essential when freezing is used to make materials (ice-templating) with unidirectional porosity.

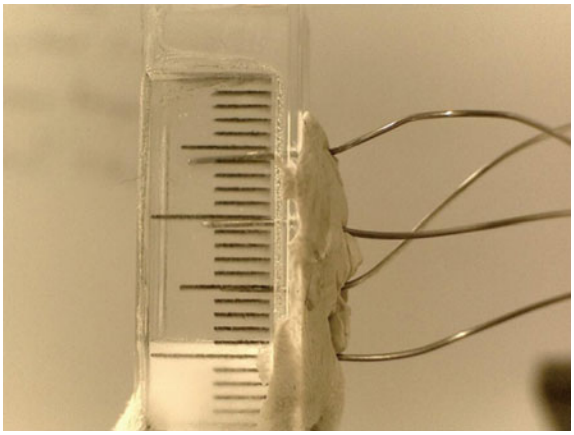

Fig. 2.35 Experimental set-up to track the freeze front in a colloidal suspensions. The mould is transparent so that the front position can be recorded. Four temperature sensors are placed in the suspension to record the time-lapse evolution of the temperature profile. From [1], Advanced Engineering Materials.

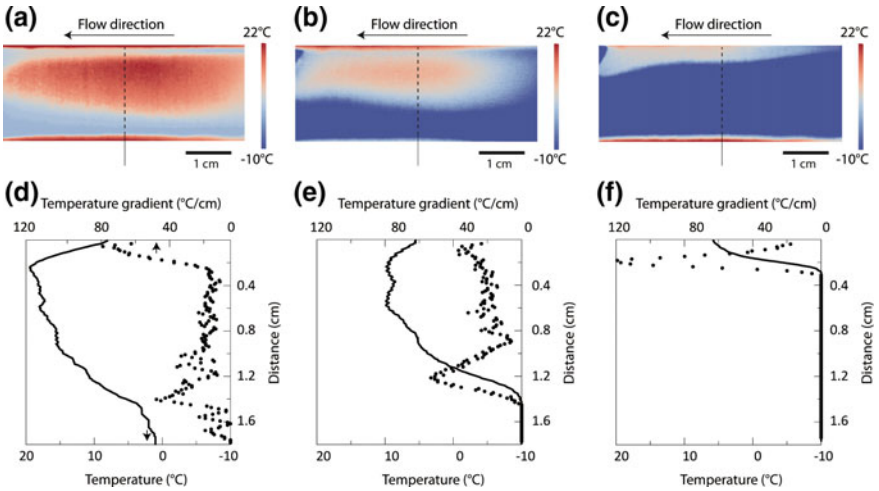

Fig. 2.36 Thermal measurements during freezing under flow. A thermal camera was used to image the temperature distribution. The temperature gradient through the sample can be obtained from these images. Reprinted from F. Bouville et al. Journal of the American Ceramic Society, Wiley [80] © 2014 The American Ceramic Society

Temperature Probe

Temperature sensors have been used to follow the time-lapse evolution of the temperature profile [76–79] (Fig. 2.35). Although such measurements can be used to track the initial stages of nucleation and growth (when an important latent heat is released), it has been mostly used to compare the temperature evolution with that predicted by the analytical models (such as the Stefan model) [1].

Thermal Camera

A thermal camera is useful to image the temperature gradient and assess how homogeneous it is. This is in particular essential when developing set-ups of large dimensions (several centimetres). However, this has been almost never reported in studies. The only image so far (Fig. 2.36) is related to the development of the freezing under flow set-up [80].

Differential Scanning Calorimetry

Differential scanning calorimetry (DSC) is extensively used to investigate phase transitions in materials science. It has thus been applied to freezing colloids. In most studies, DSC was used to measure the freezing and melting point of the suspensions [77, 81–94]. The results are discussed in Chap. 3.[2]

[2] See p. 97.

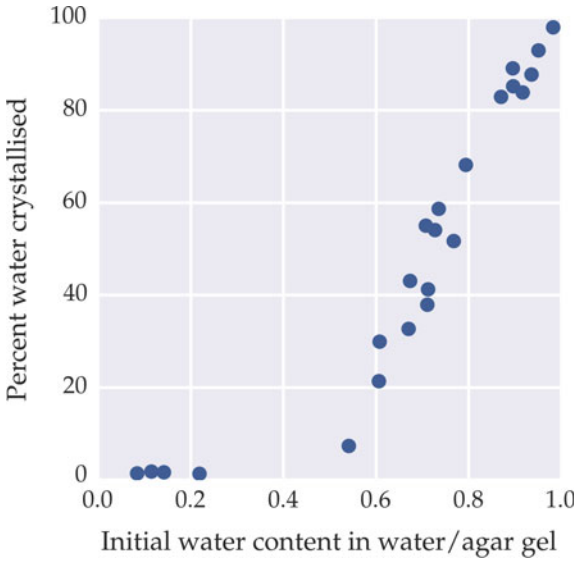

Fig. 2.37 Measurement of the fraction of water crystallised during freezing as a function of the initial water content of the water–agar gel. Replotted from [92]. The results were obtained with DSC. The trend is similar to that measured in frozen sludge [98]

DSC was also used to determine the phase diagram of systems where several solvents are present, such as water/TBA [95, 96]. The effect of additives (such as cryoprotectants) on the freezing point was also reported [97].

Beyond materials science studies, DSC was also used to investigate the freezing behaviour of sludge [98].

A precise measurement of the latent heat during freezing and thawing can be used to estimate the percentage of solvent that cannot be frozen in a system (also called bound water) (Fig. 2.37), although this has rarely been reported [92, 98].

2.7 Conclusions

Many experimental techniques have been used to investigate the freezing of colloids. Several reasons explain this diversity: the different time and space scales at which mechanisms are taking place, the variety of features of interest (thermal, electrical, optical), but also the diversity of fields or domains within which these phenomena are investigated. Magnetic resonance imaging, for instance, is commonly used in food engineering, but not so much in materials science. Again, some cross-fertilisation between the different domains would certainly expand the variety of approaches used, with benefits for everyone.

Although many space and time scales are of interest, there is a relatively narrow range where direct observations would be currently required. The range corresponds to colloidal dimensions (a few micrometres or less) and crystal growth rates (a few to a few tens of micrometres per second) encountered during most of the occurrences of

freezing colloids, and in particular in materials science (ice-templating conditions). Ideally, one wants to observe particle redistribution, solutes concentration gradients, and crystal growth in real time, without introducing artefacts. Confocal microscopy is probably the most relevant technique to explore these domains.

Finally, little has been done on the temperature-related measurements. Although DSC was used to measure the freezing and melting point, or temperature probes inserted in the suspension to follow the cooling behaviour, more precise characterisation of the development of temperature gradients would be helpful to understand and optimise the set-ups and cooling conditions.

References

1. C. Stolze, T. Janoschka, U.S. Schubert, F.A. Müller, S. Flauder, Adv. Eng. Mater. **18**(1), 111 (2016). doi:10.1002/adem.201500235
2. H. Pruppacher, J. Glaciol. **6**(47), 651 (1967)
3. D.L. Feltham, J. Geophys. Res. **107**(C2), 3009 (2002). doi:10.1029/2000JC000559
4. S. Omenyi, A. Neumann, J. Appl. Phys. (1976)
5. J. Cissé, J. Cryst. Growth **10**(1), 67 (1971). doi:10.1016/0022-0248(71)90047-9
6. B. Dutta, M.K. Surappa, Metall. Mater. Trans. A **29**(4), 1329 (1998). doi:10.1007/s11661-998-0259-y
7. G. Wilde, M. Byrnes, J. Perepezko, J. Non. Cryst. Solids **250–252**(2), 626 (1999). doi:10.1016/S0022-3093(99)00148-9
8. H. Ishiguro, B. Rubinsky, Cryobiology **31**(5), 483 (1994). doi:10.1006/cryo.1994.1059
9. P. Casses, A. Azouni, Int. Commun. Heat Mass Transf. **22**(4), 605 (1995)
10. C. Körber, M. Rau et al., J. Cryst. Growth **72**(3), 649 (1985)
11. G. Lipp, C. Körber, G. Rau, J. Cryst. Growth **99**(1–4), 206 (1990)
12. K. Jackson, J. Hunt, Acta Metall. **13**(11), 1212 (1965). doi:10.1016/0001-6160(65)90061-1
13. I. Farup, J.M. Drezet, M. Rappaz, Acta Mater. **49**(7), 1261 (2001). doi:10.1016/S1359-6454(01)00013-1
14. H. Xing, J.Y. Wang, C.L. Chen, Z.F. Shen, C.W. Zhao, J. Cryst. Growth **338**(1), 256 (2012). doi:10.1016/j.jcrysgro.2011.10.047
15. A.M. Anderson, M.G. Worster, Langmuir **28**(48), 16512 (2012). doi:10.1021/la303458m
16. Y. Suzuki, G. Sazaki, K. Hashimoto, T. Fujiwara, Y. Furukawa, J. Cryst. Growth **383**, 67 (2013). doi:10.1016/j.jcrysgro.2013.08.026
17. J. You, L. Wang, Z. Wang, J. Li, J. Wang, X. Lin, W. Huang, Rev. Sci. Instrum. **86**(8), 084901 (2015). doi:10.1063/1.4928108
18. J.M.H. Schollick, R.W. Style, A. Curran, J.S. Wettlaufer, E.R. Dufresne, P.B. Warren, K.P. Velikov, R.P.A. Dullens, D.G.A.L. Aarts, J. Phys. Chem. B **120**(16), 3941 (2016). doi:10.1021/acs.jpcb.6b00742
19. S.S. Peppin, J.S. Wettlaufer, M.G. Worster, Phys. Rev. Lett. **100**(23), 1 (2008). doi:10.1103/PhysRevLett.100.238301
20. S.S. Peppin, J.A.W. Elliott, M.G. Worster, J. Fluid Mech. **554**(1), 147 (2006). doi:10.1017/S0022112006009268
21. S.S. Peppin, M.G. Worster, J.S. Wettlaufer, Proc. R. Soc. A Math. Phys. Eng. Sci. **463**(2079), 723 (2007). doi:10.1098/rspa.2006.1790
22. A.M. Anderson, M. Grae Worster, J. Fluid Mech. **758**, 786 (2014). doi:10.1017/jfm.2014.500
23. L. Wang, J. You, Z. Wang, J. Wang, X. Lin, Sci. Rep. **6**, 23358 (2016). doi:10.1038/srep23358
24. J. You, L. Wang, Z. Wang, J. Li, J. Wang, X. Lin, W. Huang, Sci. Rep. **6**, 28434 (2016). doi:10.1038/srep28434

25. A. Bogner, G. Thollet, D. Basset, P.H. Jouneau, C. Gauthier, Ultramicroscopy **104**(3–4), 290 (2005). doi:10.1016/j.ultramic.2005.05.005
26. M.L. Ferrer, R. Esquembre, I. Ortega, C.R. Mateo, F. del Monte, Chem. Mater. **18**(2), 554 (2006). doi:10.1021/cm052087z
27. A.E. Donius, R.W. Obbard, J.N. Burger, P.M. Hunger, I. Baker, R.D. Doherty, U.G.K. Wegst, Mater. Charact. **93**, 184 (2014). doi:10.1016/j.matchar.2014.04.003
28. P. Prado, B. Balcom, S. Beyea, T. Bremner, R. Armstrong, P. Grattan-Bellew, Cem. Concr. Res. **28**(2), 261 (1998). doi:10.1016/S0008-8846(97)00222-6
29. W.L. Kerr, R.J. Kauten, M.J. McCarthy, D.S. Reid, LWT - Food Sci. Technol. **31**(3), 215 (1998). doi:10.1006/fstl.1997.0323
30. H. Eicken, C. Bock, R. Wittig, H. Miller, H.O. Poertner, Cold Reg. Sci. Technol. **31**(3), 207 (2000). doi:10.1016/S0165-232X(00)00016-1
31. P. Aussillous, A. Sederman, L. Gladden, H. Huppert, M.G. Worster, in *XXI ICTAM* (2004)
32. M.K. Lee, M.H. Rich, A. Shkumatov, J.H. Jeong, M.D. Boppart, R. Bashir, M.U. Gillette, J. Lee, H. Kong, Adv. Healthc. Mater. **4**(2), 195 (2015). doi:10.1002/adhm.201400153
33. G. Do, T. Araki, Y. Bae, K. Ishikura, Y. Sagara, Dry. Technol. **33**(13), 1614 (2015). doi:10.1080/07373937.2015.1029073
34. G.E. Sosinsky, J. Crum, Y.Z. Jones, J. Lanman, B. Smarr, M. Terada, M.E. Martone, T.J. Deerinck, J.E. Johnson, M.H. Ellisman, J. Struct. Biol. **161**(3), 359 (2008)
35. R.J. Mikula, V.A. Munoz, Colloids Surf. **174**, 23 (2000)
36. J. Du, R.A. Pushkarova, R.S. Smart, Int. J. Miner. Process. **93**(1), 66 (2009). doi:10.1016/j.minpro.2009.06.004
37. C.L. Zhao, S. Porzio, A. Smith, H. Ge, H.T. Davis, L.E. Scriven, J. Coat. Technol. Res. **3**(2), 109 (2006). doi:10.1007/s11998-006-0013-6
38. A. Lasalle, C. Guizard, S. Deville, F. Rossignol, P. Carles, J. Am. Ceram. Soc. **94**(1), 244 (2011). doi:10.1111/j.1551-2916.2010.04034.x
39. D. Studer, M. Michel, M. Wohlwend, E.B. Hunziker, M.D. Buschmann, J. Microsc. **179**(Pt 3), 321 (1995)
40. M.F. Butler, Cryst. Growth Des. **2**(6), 541 (2002)
41. S. Deville, E. Maire, G. Bernard-Granger, A. Lasalle, A. Bogner, C. Gauthier, J. Leloup, C. Guizard, Nat. Mater. **8**(12), 966 (2009). doi:10.1038/nmat2571
42. S. Deville, E. Maire, A. Lasalle, A. Bogner, C. Gauthier, J. Leloup, C. Guizard, J. Am. Ceram. Soc. **92**(11), 2497 (2009). doi:10.1111/j.1551-2916.2009.03264.x
43. S. Deville, E. Maire, A. Lasalle, A. Bogner, C. Gauthier, J. Leloup, C. Guizard, J. Am. Ceram. Soc. **92**(11), 2489 (2009). doi:10.1111/j.1551-2916.2009.03163.x
44. S. Deville, E. Maire, A. Lasalle, A. Bogner, C. Gauthier, J. Leloup, C. Guizard, J. Am. Ceram. Soc. **93**(9), 2507 (2010). doi:10.1111/j.1551-2916.2010.03840.x
45. A. Lasalle, C. Guizard, E. Maire, J. Adrien, S. Deville, Acta Mater. **60**(11), 4594 (2012). doi:10.1016/j.actamat.2012.02.023
46. B. Delattre, H. Bai, R.O. Ritchie, J. De Coninck, A.P. Tomsia, A.C.S. Appl, Mater. Interfaces **6**(1), 159 (2014). doi:10.1021/am403793x
47. D.F. Souza, E.H. Nunes, D.S. Pimenta, D.C. Vasconcelos, J.F. Nascimento, W. Grava, M. Houmard, W.L. Vasconcelos, Mater. Charact. **96**, 183 (2014). doi:10.1016/j.matchar.2014.08.009
48. A. Bareggi, E. Maire, A. Lasalle, S. Deville, J. Am. Ceram. Soc. **94**(10), 3570 (2011). doi:10.1111/j.1551-2916.2011.04572.x
49. S. Deville, J. Adrien, E. Maire, M. Scheel, M. Di Michiel, M.D. Michiel, Acta Mater. **61**(6), 2077 (2013). doi:10.1016/j.actamat.2012.12.027
50. C.A. Schneider, W.S. Rasband, K.W. Eliceiri, Nat. Methods **9**(7), 671 (2012). doi:10.1038/nmeth.2089
51. J. Schindelin, I. Arganda-Carreras, E. Frise, V. Kaynig, M. Longair, T. Pietzsch, S. Preibisch, C. Rueden, S. Saalfeld, B. Schmid, J.Y. Tinevez, D.J. White, V. Hartenstein, K. Eliceiri, P. Tomancak, A. Cardona, Nat. Methods **9**(7), 676 (2012). doi:10.1038/nmeth.2019

52. S. van der Walt, J.L. Schönberger, J. Nunez-Iglesias, F. Boulogne, J.D. Warner, N. Yager, E. Gouillart, T. Yu, PeerJ **2**, e453 (2014). doi:10.7717/peerj.453
53. D.B. Hovis, A.H. Heuer, J. Microsc. **240**(3), 173 (2010). doi:10.1111/j.1365-2818.2010.03399.x
54. P.J. Lu, Gelation and Phase Separation of Attractive Colloids. Ph.D. thesis, Harvard University (2008)
55. V. Prasad, D. Semwogerere, E.R. Weeks, J. Phys. Condens. Matter **19**(11), 113102 (2007). doi:10.1088/0953-8984/19/11/113102
56. E.R. Weeks, C. Nugent, Rep. Inst. Fluid Sci. **19** (2007)
57. U. Gasser, E.R. Weeks, A.B. Schofield, P.N. Pusey, D.A. Weitz, Science **292**, 258 (2001)
58. L. Ma, Biomaterials **24**(26), 4833 (2003). doi:10.1016/S0142-9612(03)00374-0
59. G. Kumaraswamy, B. Biswas, C.K. Choudhury, Faraday Discuss. **186**, 61 (2016). doi:10.1039/C5FD00125K
60. M. Marcellini, C. Noirjean, D. Dedovets, J. Maria, S. Deville, ACS Omega (2016). doi:10.1021/acsomega.6b00217
61. P.L. Gai, Microsc. Microanal. **8**(1), 21 (2002). doi:10.1017/S1431927601010054
62. E.R. White, M. Mecklenburg, B. Shevitski, S.B. Singer, B.C. Regan, Langmuir **28**(8), 3695 (2012). doi:10.1021/la2048486
63. K. Tai, Y. Liu, S.J. Dillon, Microsc. Microanal. **20**(2), 330 (2014). doi:10.1017/S1431927613014128
64. S. Piazolo, M. Montagnat, J.R. Blackford, J. Microsc. **230**(3), 509 (2008). doi:10.1111/j.1365-2818.2008.02014.x
65. I. Weikusat, D.A.M. de Winter, G.M. Pennock, M. Hayles, C.T.W.M. Schneijdenberg, M.R. Drury, J. Microsc. **242**(3), 295 (2011). doi:10.1111/j.1365-2818.2010.03471.x
66. R. Obbard, J. Glaciol. **52**(179), 546 (2006). doi:10.3189/172756506781828458
67. M. Montagnat, J.R. Blackford, S. Piazolo, L. Arnaud, R.A. Lebensohn, Earth Planet. Sci. Lett. **305**(1–2), 153 (2011). doi:10.1016/j.epsl.2011.02.050
68. D.J. Prior, S. Diebold, R. Obbard, C. Daghlian, D.L. Goldsby, W.B. Durham, I. Baker, Scr. Mater. **66**(2), 69 (2012). doi:10.1016/j.scriptamat.2011.09.044
69. D. Prior, K. Lilly, M. Seidemann, M. Vaughan, L. Becroft, R. Easingwood, S. Diebold, R. Obbard, C. Daghlian, I. Baker, T. Caswell, N. Golding, D. Goldsby, W. Durham, S. Piazolo, C. Wilson, J. Microsc. **259**(3), 237 (2015). doi:10.1111/jmi.12258
70. S. Deville, C. Viazzi, J. Leloup, A. Lasalle, C. Guizard, E. Maire, J. Adrien, L. Gremillard, PLOS One **6**(10), e26474 (2011). doi:10.1371/journal.pone.0026474
71. D.B. Varshney, J.A. Elliott, L.A. Gatlin, S. Kumar, R. Suryanarayanan, E.Y. Shalaev, J. Phys. Chem. B **113**(18), 6177 (2009). doi:10.1021/jp900404m
72. G. Gupta, R.F. Rice, W.R. Wilcox, J. Colloid Interface Sci. **82**(2), 458 (1981). doi:10.1016/0021-9797(81)90387-8
73. G. Lecomte-Nana, V. Coudert, F. Rossignol, A. Lasalle, J. Am. Ceram. Soc. **95**(6), 1883 (2012). doi:10.1111/j.1551-2916.2012.05154.x
74. M. Spannuth, S.G.J. Mochrie, S.S. Peppin, J.S. Wettlaufer, Phys. Rev. E **83**(2), 32 (2011). doi:10.1103/PhysRevE.83.021402
75. M. Spannuth, S.G.J. Mochrie, S.S. Peppin, J.S. Wettlaufer, J. Chem. Phys. **135**(22), 224706 (2011). doi:10.1063/1.3665927
76. D. Koch, L. Andresen, T. Schmedders, G. Grathwohl, J. Sol-Gel Sci. Technol. **26**(1–3), 149 (2003). doi:10.1023/A:1020718225164
77. H. Liu, K. Nakagawa, D. Chaudhary, Y. Asakuma, M.O. Tadé, Chem. Eng. Res. Des. **89**(11), 2356 (2011). doi:10.1016/j.cherd.2011.02.023
78. P.M. Hunger, A.E. Donius, U.G.K. Wegst, Acta Biomater. **9**(5), 6338 (2013). doi:10.1016/j.actbio.2013.01.012
79. C. Stolze, T. Janoschka, S. Flauder, F.A. Müller, M.D. Hager, U.S. Schubert, A.C.S. Appl, Mater. Interfaces **8**(36), 23614 (2016). doi:10.1021/acsami.6b05018
80. F. Bouville, E. Portuguez, Y. Chang, G. Messing, A.J. Stevenson, E. Maire, L. Courtois, S. Deville, J. Am. Ceram. Soc. **97**(6), 1736 (2014). doi:10.1111/jace.12976

81. B.H. Yoon, Y.H. Koh, C.S. Park, H.E. Kim, J. Am. Ceram. Soc. **90**(6), 1744 (2007). doi:10.1111/j.1551-2916.2007.01670.x
82. S.W. Yook, H.E. Kim, Y.H. Koh, Mater. Lett. **63**(17), 1502 (2009). doi:10.1016/j.matlet.2009.03.056
83. Y.M. Soon, K.H. Shin, Y.H. Koh, J.H. Lee, H.E. Kim, Mater. Lett. **63**(17), 1548 (2009). doi:10.1016/j.matlet.2009.04.013
84. X. Liu, M.N. Rahaman, Q. Fu, Acta Biomater. **7**(1), 406 (2011). doi:10.1016/j.actbio.2010.08.025
85. M.C. Yang, J.S. Perng, J. Membr. Sci. **187**(1–2), 13 (2001). doi:10.1016/S0376-7388(00)00587-1
86. S.W. Yook, B.H. Yoon, H.E. Kim, Y.H. Koh, Y.S. Kim, Mater. Lett. **62**(30), 4506 (2008). doi:10.1016/j.matlet.2008.08.010
87. B.H. Yoon, E.J. Lee, H.E. Kim, Y.H. Koh, J. Am. Ceram. Soc. **90**(6), 1753 (2007). doi:10.1111/j.1551-2916.2007.01703.x
88. S.E. Naleway, C.F. Yu, M.M. Porter, A. Sengupta, P.M. Iovine, M.A. Meyers, J. McKittrick, Mater. Des. **71**, 62 (2015). doi:10.1016/j.matdes.2015.01.010
89. Y. Tang, S. Qiu, C. Wu, Q. Miao, K. Zhao, J. Eur. Ceram. Soc. **36**(6), 1513 (2016). doi:10.1016/j.jeurceramsoc.2015.12.047
90. A. Lasalle, C. Guizard, J. Leloup, S. Deville, E. Maire, A. Bogner, C. Gauthier, J. Adrien, L. Courtois, J. Am. Ceram. Soc. **95**(2), 799 (2012). doi:10.1111/j.1551-2916.2011.04993.x
91. K. Nakagawa, S. Surassmo, S.G. Min, M.J. Choi, J. Food Eng. **102**(2), 177 (2011). doi:10.1016/j.jfoodeng.2010.08.017
92. H.M. Tong, I. Noda, C.C. Gryte, Colloid Polym. Sci. **262**(7), 589 (1984). doi:10.1007/BF01451524
93. P.T.N. Nguyen, J. Ulrich, Chem. Eng. Technol. **37**(8), 1376 (2014). doi:10.1002/ceat.201400032
94. P. Nguyen, J. Ulrich, J. Food Eng. **153**, 1 (2015). doi:10.1016/j.jfoodeng.2014.12.007
95. K. Kasraian, P.P. DeLuca, Pharm. Res. **12**(4), 484 (1995). doi:10.1023/A:1016233408831
96. A. Borisova, M. De Bruyn, V.L. Budarin, P.S. Shuttleworth, J.R. Dodson, M.L. Segatto, J.H. Clark, Macromol. Rapid Commun. **36**(8), 774 (2015). doi:10.1002/marc.201400680
97. P.F. Yue, G. Li, J.X. Dan, Z.F. Wu, C.H. Wang, W.F. Zhu, M. Yang, Int. J. Pharm. **475**(1–2), 35 (2014). doi:10.1016/j.ijpharm.2014.08.041
98. G. Ezekwo, H.M. Tong, C.C. Gryte, Water Res. **14**(8), 1079 (1980). doi:10.1016/0043-1354(80)90156-6

http://www.springer.com/978-3-319-50513-8

Freezing Colloids: Observations, Principles, Control, and Use

Applications in Materials Science, Life Science, Earth Science, Food Science, and Engineering

Deville, S.

2017, XXIII, 598 p. 365 illus., Hardcover

ISBN: 978-3-319-50513-8